Journal of Oceanography
Vol. 50, pp. 559 to 588. 1994

Winter Water Mass Distributions in the Western Gulf of Mexico Affected by a Colliding Anticyclonic Ring

VÍCTOR M. V. VIDAL, FRANCISCO V. VIDAL, ABEL F. HERNÁNDEZ, EUSTORGIO MEZA and LORENZO ZAMBRANO

Grupo de Estudios Oceanográficos, Instituto de Investigaciones Eléctricas, Apdo. Postal 475, Cuernavaca, Morelos, 62000 México

(Received 21 September 1993; in revised form 23 May 1994; accepted 27 May 1994)

The winter water mass distributions in the western Gulf of Mexico, affected by the collision of a Loop Current anticyclonic ring, during January 1984 are analyzed. Two principal modes of Gulf Common Water (GCW) formation, arising from the dilution of the Caribbean Subtropical Underwater (SUW), are identified. Within the western gulf continental slope to the east of Tamiahua, the GCW is formed by the collision of anticyclonic rings. During these collision events, the SUW, entrapped at the core (200 m depth) of these features, is diluted by low salinity ($36.1 \leq S \leq 36.3$‰) water from the uppermost layer of the main thermocline. The end product of this mixture is GCW, which is further diluted by low salinity coastal water within the western gulf continental shelf. The second GCW formation mode is associated to the northerly wind stress which propagates over the western gulf during winter. During January, 1984, this wind stress gave rise to a 175 m mixed layer. This convective mixing destroyed the static stability of the summer thermocline and allowed for the partial dilution of the SUW with low salinity ($S \leq 36.3$‰) water from the western gulf continental shelf. Within the western gulf's upper 2000 m, the following water masses were identified to be present: GCW, SUW, Tropical Atlantic Central Water and associated dissolved oxygen minimum stratum, Antarctic Intermediate Water remnant, a mixture of the Caribbean Intermediate Water and the upper portion of North Atlantic Deep Water (NADW), and the NADW itself. The topographic distribution of these water masses' strata was dictated by the cyclonic-anticyclonic baroclinic circulation that evolved from the anticyclone's collision to the east of Tamiahua. Between the cyclonic and anticyclonic domains, the maximum pressure differential of these water masses' core occurrences was 150 to 280 dbar. The topographic transition zone defined by these strata occurred between the cyclonic and anticyclonic domains and coincided unambiguously with the anticyclone's collision zone. Within the continental shelf, we identified low temperature (12°C) and low salinity (31‰) coastal waters contributed by river runoff. Driven by the northerly wind stress, these coastal waters were advected toward the south hugging the coastline. The coastal and continental shelf waters demarcated a sea surface temperature, salinity, and dissolved oxygen discontinuity region that coincided with the horizontal baroclinic flow transition zone associated to the anticyclone's collision.

1. Introduction

The water mass distributions in the western Gulf of Mexico have been sparsely documented.

A characterization of the Gulf of Mexico waters during winter was reported by McLellan and Nowlin (1963), Nowlin and McLellan (1967), and Nowlin (1972). Morrison *et al.* (1983) analyzed the distributions of salinity, dissolved oxygen, nitrate, phosphate, and silicate for the western Gulf of Mexico in 1978 and identified the principal water masses occurring within the western gulf. Elliott (1979, 1982) and Vidal *et al.* (1989, 1990, 1994) have shown that the hydrographic properties and water masses distributions in the Gulf of Mexico are determined by the presence of cyclonic and anticyclonic rings.

Vidal *et al.* (1989, 1992) have shown that Loop Current anticyclones, which collide against the western gulf continental slope, have a determinant effect in the formation of the Gulf Common Water (GCW; $S = 36.3$ to 36.4‰; $T \approx 22.5$°C). The GCW formation mechanism identified by Vidal *et al.* (1989, 1992) is driven by the anticyclones' shedding approximately one third of their volume ($\sim 2 \times 10^4$ km^3) during their collisions to flanking cyclones, that are formed at the peripheries of the anticyclones. Two important questions have yet to be answered. Which are the principal modes of GCW formation in the gulf? And what happens to the water mass distributions in the western gulf during these collision events?

In this paper, we attempt to answer these questions by analyzing the hydrography and water mass distributions within the upper 2000 dbar in the western Gulf of Mexico during the collision event of an anticyclonic ring reported by Vidal *et al.* (1992). The hydrographic data utilized in our analyses were collected from January 6 to 30, 1984, aboard R/V *Justo Sierra* on cruise Argos 84-1 (Vidal *et al.*, 1985a, 1986, 1989).

Lewis and Kirwan (1985) have reported on Lagrangian measurements of drifters that were seeded in Loop Current anticyclonic rings and tracked their migrations and interactions in the western Gulf of Mexico. Figures 1(b) and 1(c) of Lewis and Kirwan (1985) show that ring 3374, which broke off the Loop Current in June 1982, started interacting with the western gulf continental slope nine months later, in March 1983, and its collision persisted for at least five months. On the other hand, the Lagrangian trajectory of drifter 3375, which appears in Fig. 2(a) of Lewis and Kirwan (1985), clearly reveals the interaction of an anticyclonic ring (probably 3374) with the western gulf continental slope from August 10, 1983 to February 29, 1984. We believe this is the anticyclonic ring collision we sampled and studied during the Argos 84-1 cruise. The Lagrangian trajectory of drifter 3375 and its residence time within the western gulf coincide with the time frame and spatial coverage of our hydrographic sampling. Although our hydrographic station distribution coincides with the Lagrangian track of drifter 3375, it should also be mentioned that Cooper *et al.* (1990) reported the presence of a 200 km in diameter anticyclonic ring (Big Eddy) which had pinched off the Loop Current in July or August 1983 and probably hit the western shelf off Brownsville, at 26°N, 96°W, sometime in November or December 1983. Our Argos 84-1 hydrographic measurements, from 25° to 26°N and 95° to 96°W, most likely sampled the western section of Big Eddy.

2. Field Measurements and Data Reduction

The Argos 84-1 hydrographic stations grid is shown in Fig. 1(a). Cruise transects and hydrographic stations' identification numbers and positions are shown in Fig. 1(b). A total of 76 hydrographic stations were occupied along 11 latitudinal transects from 25°55′ N (Matamoros) to 19°20′ N (Veracruz). Hydrographic stations were purposely positioned to sample the western Gulf of Mexico continental shelf water mass as well as its continental slope and deep water masses. The deepest hydrographic casts reached 2000 dbar (Vidal *et al.*, 1985a, 1986, 1989).

The conductivity-temperature-pressure (CTD) hydrocasts undertaken from the R/V *Justo*

Sierra utilized a Neil Brown CTD Mark III probe. The CTD sensors were mounted 1 m below a 12-bottle General Oceanics Rosette sampler fitted with 1.5 L Niskin bottles.

Water samples were collected at each station and used to calibrate the CTD sensors following the data processing techniques of Fofonoff *et al.* (1974), Millard (1982), and Millard and Galbraith (1982). The CTD-Rosette unit was stopped at predetermined sampling depths during ascent to the surface and a bottle was closed at each level. The CTD analog output recorded during the probe's descent and ascent was used to sample known water masses, thus, enhancing the CTD sensors' calibration.

Salinity water samples were analyzed on board, under laboratory-controlled temperature conditions, using a Guildline Model 8400 salinometer. Under these conditions, a precision of ±0.001 practical salinity units is achievable (Mantyla, 1980). Dissolved oxygen concentrations were determined using the Winkler method described by Strickland and Parsons (1972). On-cruise calibration of salinity and dissolved oxygen concentrations were obtained from triplicate analysis of seawater samples at each hydrographic station. The uncertainties in these determinations were 0.002‰ for salinity and 0.022 mL L^{-1} for dissolved oxygen.

The calibrated CTD data were averaged over 2-dbar blocks and these regularly spaced data formed the basis for all subsequent calculations. Density was computed utilizing the new international equation of state for seawater (EOS 80), following the UNESCO algorithms of Fofonoff and Millard (1983) and Fofonoff (1985). Data points between hydrographic stations were interpolated by bilinear interpolation, quadratic interpolation, and by distance weighting methods (IMSL Mathematical Library, 1987).

3. Baroclinic Circulation

Vidal *et al.* (1992) analyzed the baroclinic circulation in the western Gulf of Mexico during January 1984. They showed that within the western gulf oceanic region the baroclinic circulation, induced by the presence and collision of an anticyclonic Loop Current ring, determined the distribution of hydrographic properties and dominated over the ageostrophic current component induced by the northerly wind stress. These observations are consistent with the acoustic profile current (ADCP) measurements made in December 1983, within the northwestern sector (24.5° to 26.5°N and 94.8° and 95.7°W) of our study area, by Cooper *et al.* (1990). Their ADCP measurements, conducted three weeks before the Argos 84-1 cruise, revealed peak currents near 1 m s^{-1}, at 100 dbar, in a 200 km in diameter anticyclone (Big Eddy). Their geostrophic velocity estimates, calculated along different sectors of this ring, were of the order of 30 to 134 cm s^{-1}.

The dynamic topography distribution of the western Gulf of Mexico referenced to 500 dbar is shown in Fig. 2(a). The dynamic topography to the west of the 500 m isobath represents an extrapolation of the geopotential height in the eastern region's study area. The baroclinic circulation derived from this geopotential height distribution is shown in Fig. 2(b). From these two figures one can observe a transition zone, to the east of Tamiahua, where the surface baroclinic circulation diverges into north and south currents that flow parallel to the shelf break. The sea surface baroclinic currents that diverge to the north have maximum speeds of 80 cm s^{-1} and are stronger than those that diverge to the south and which have maximum speeds of 26 cm s^{-1}.

The dynamic topography relative to 500 dbar, shown in Fig. 2(a), reveals two distinct zones, one of maximum geopotential height located to the east of Matamoros, at 26°00′ N, 95°00′ W, and one of minimum geopotential height located to the northeast of Veracruz, at 20°00′ N, 95°00′ W. These dynamic topography distributions are diametrically opposite with each other. To the

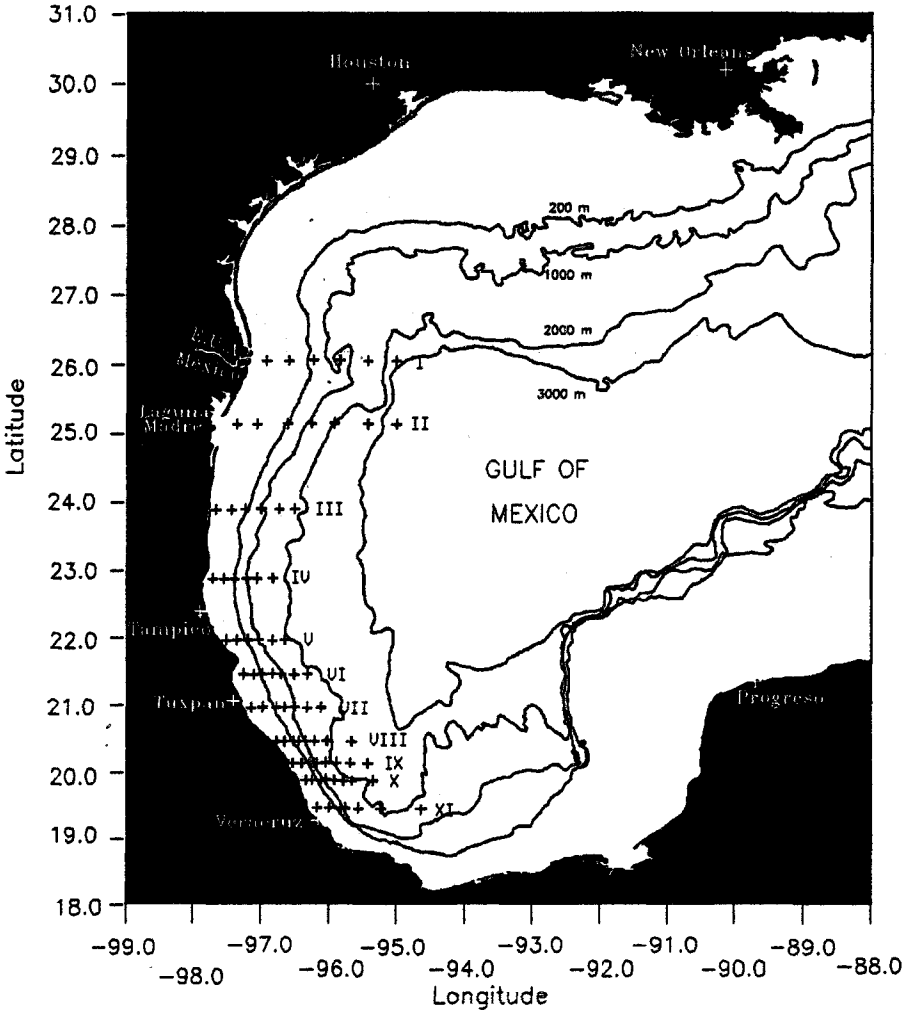

Fig. 1. (a) The Gulf of Mexico and its bathymetry. Argos 84-1 study area and hydrographic station distribution. (b) Argos 84-1 cruise transects and hydrographic station identification (after Vidal *et al.*, 1992).

north of 23°N the geopotential height increases toward the east, while to the south of 21°N the geopotential height increases toward the west (Fig. 2(a)).

In Fig. 3(a) we show the distribution of the baroclinic flow horizontal divergence at the sea surface referenced to 500 dbar. This current field reveals the presence of anticyclonic and convergent flow which dominates the sea surface circulation between 23° and 26°N and the presence of cyclonic and divergent flow to the south of 22°N. To the east of Tamiahua the horizontal divergence values demarcate the transition zone between convergent flow to the north and divergent flow toward the south. This horizontal divergence distribution reveals the collision of an anticyclonic ring whose translation is toward the north, moving parallel to the continental shelf break. The transition zone, to the east of Tamiahua, reveals the region and initial state of the ring collision. Within the anticyclonic ring's collision zone (21.5° to 23°N) the baroclinic

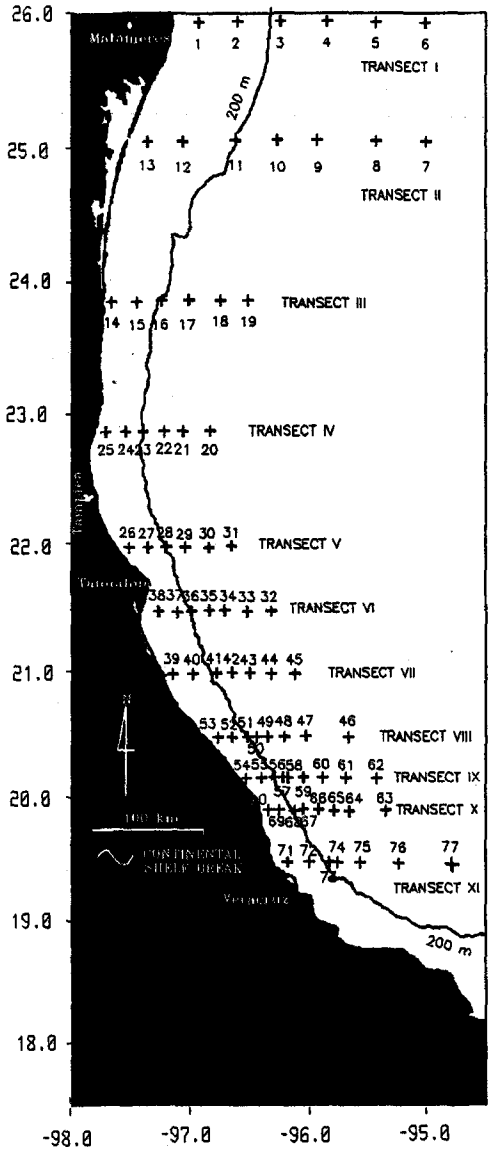

Fig. 1. (continued).

flow depicts neither convergent nor divergent flow. The horizontal divergence fluctuates from positive (2×10^{-8} s^{-1}) to negative (-2×10^{-8} s^{-1}) values, as would be expected from the unstable horizontal velocity gradients $\partial u/\partial x$ and $\partial v/\partial y$ that should develop within the collision zone. To the north and south of the collision zone the horizontal baroclinic flow stabilizes, as is shown in Figs. 2(a) and 2(b), and the horizontal divergence values become increasingly negative (-1.4×10^{-7} s^{-1}) toward the north and positive (6.0×10^{-8} s^{-1}) toward the south. Thus, the horizontal divergence distribution characterizes the anticyclonic (convergent) and cyclonic (divergent) circulation properties that dominate in each of these regions, respectively.

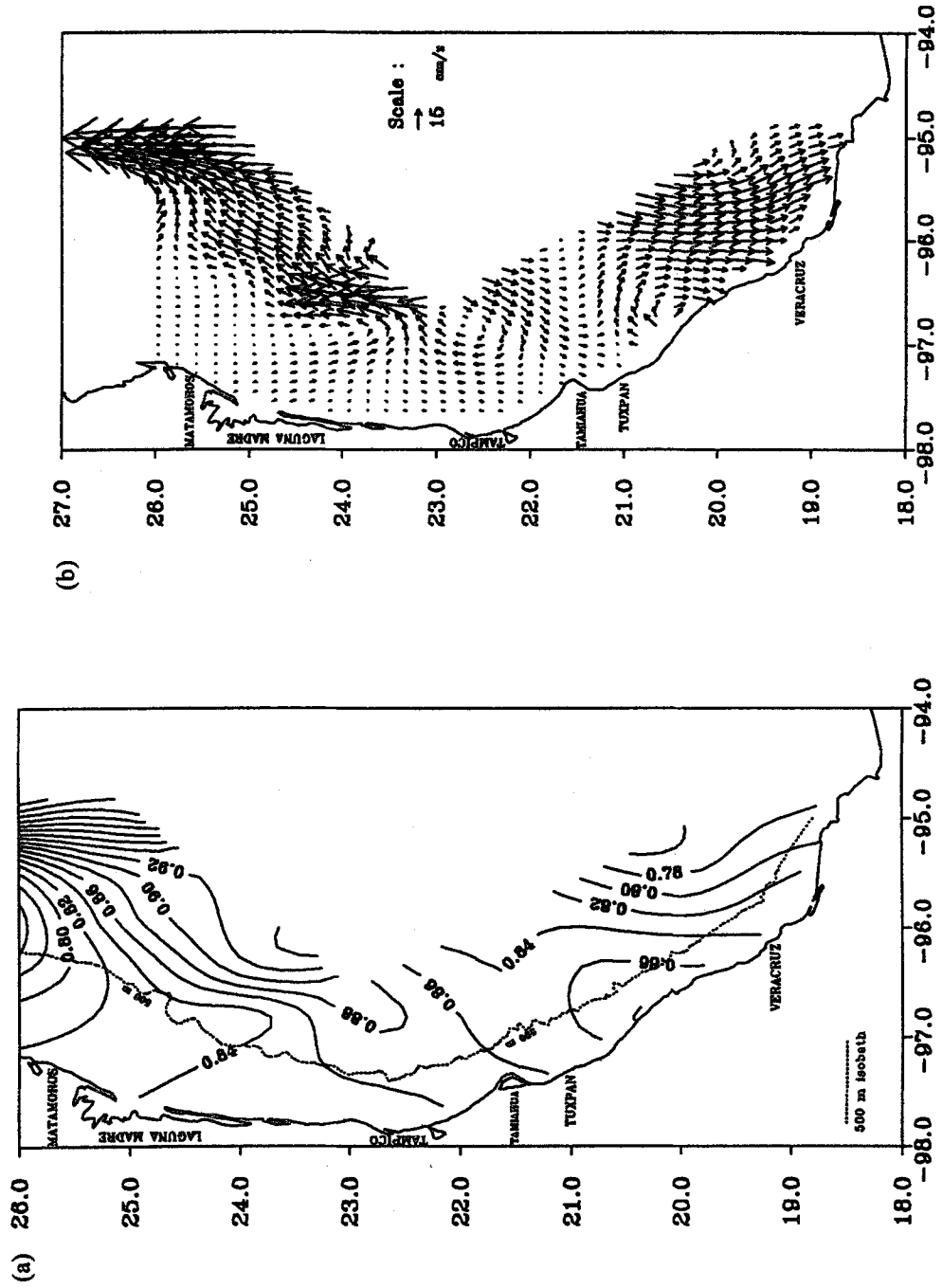

Fig. 2. (a) Extrapolated dynamic topography (dyn m) of the western Gulf of Mexico sea surface relative to 500 dbar during January 1984. (b) Extrapolated baroclinic circulation at the western Gulf of Mexico sea surface relative to 500 dbar during January 1984.

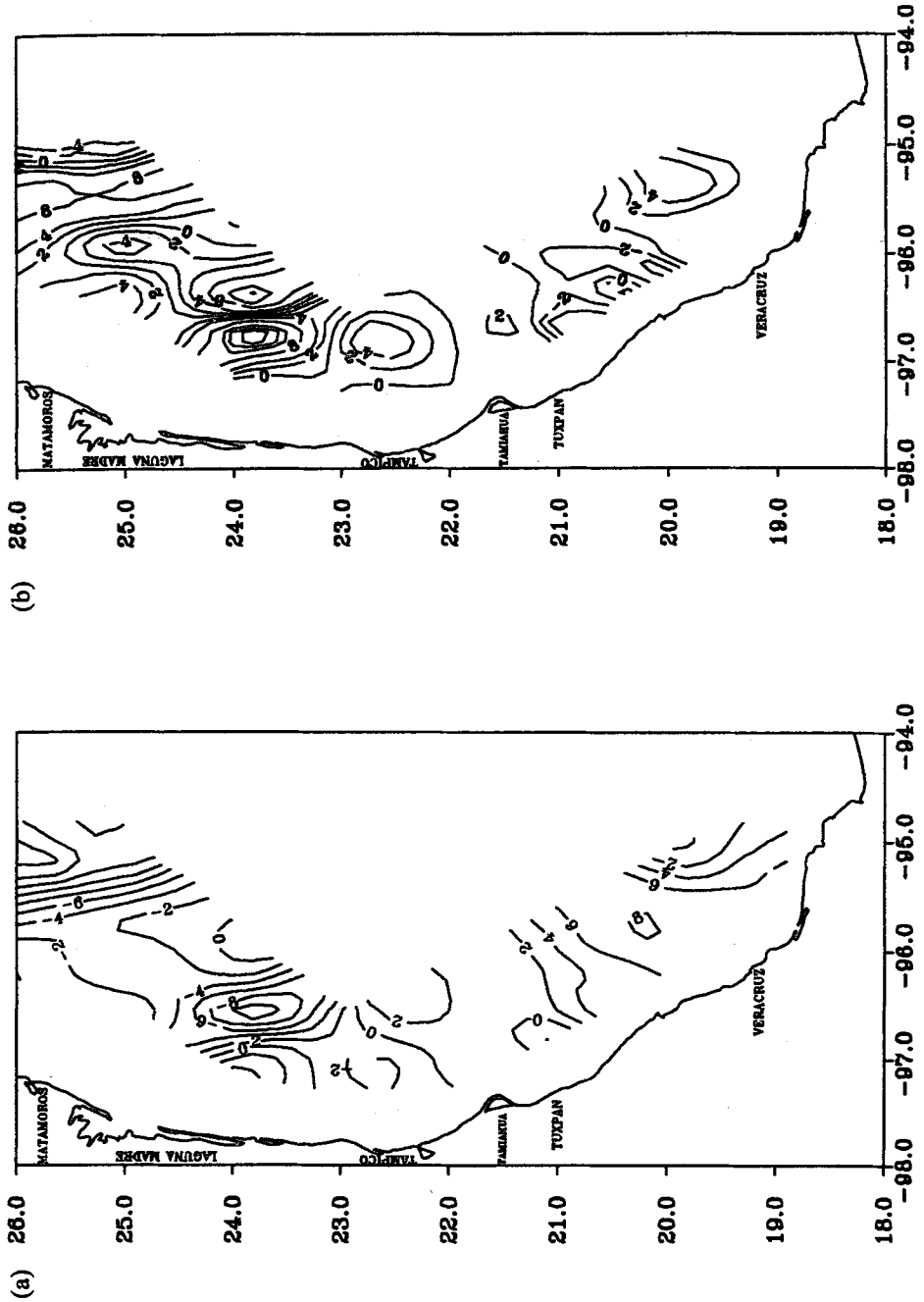

Fig. 3. (a) Horizontal divergence distribution (10^{-8} s^{-1}) at the western Gulf of Mexico sea surface, derived from the horizontal baroclinic velocity gradients relative to 500 dbar, during January 1984. (b) Vertical vorticity distribution (10^{-6} s^{-1}) at the western Gulf of Mexico sea surface, derived from the horizontal baroclinic velocity gradients relative to 500 dbar, during January 1984.

Vidal *et al.* (1992, 1994) have shown that the weakening of the anticyclonic rings' relative vorticity in the western gulf is due to their collision against the western gulf continental slope. The weakening of the anticyclonic rings' relative vorticity is made up by gain of cyclonic vorticity from lateral shear in the water current jets that flow parallel to the western continental shelf to the north and south of the anticyclones' collision zones. Hence, anticyclonic ring interactions with the western gulf boundary give rise to cyclonic-anticyclonic ring pairs. The distribution of the vertical component of relative vorticity at the sea surface referenced to 500 dbar that is shown in Fig. 3(b) is a good case in point which exemplifies these findings. Positive and negative vorticity values in Fig. 3(b) indicate cyclonic and anticyclonic circulations, respectively. Within the anticyclonic ring collision zone a weak (-6.0×10^{-6} s^{-1}, in vorticity) anticyclonic eddy is identified. This eddy is most likely a remnant or a fossil eddy that remains after the anticyclones collision event. North of the collision zone stronger cyclonic-anticyclonic circulations are identified over the continental slope at 24°00′ and 26°00′ N. It appears, from these vertical vorticity component distributions, that the northward translation of the anticyclonic ring transfers angular momentum to the water mass at its western flank originating zones of high velocity shear that develop into cyclonic eddies at the periphery of the anticyclone. South of the collision zone the cyclonic circulation is well defined at 19°30′ N, 95°30′ W, where the vertical component of vorticity is of the order of 6.0×10^{-6} s^{-1}. A weak anticyclonic eddy can also be identified over the continental shelf and shelf break, to the east of Tuxpan, which flanks the southern cyclone. It appears that the cyclone's south flowing current develops enough velocity shear to transfer angular momentum to the water mass at its western periphery to originate this anticyclonic eddy.

4. Water Masses in the Western Gulf of Mexico

4.1 Gulf Common Water formation processes

One of the principal characteristics of the western Gulf of Mexico oceanic mixed layer is the presence of the Gulf Common Water (GCW), characterized by a salinity of 36.3 to 36.4‰ and a temperature of ~22.5°C (Nowlin, 1972; Elliott, 1979, 1982; Merrell and Morrison, 1981). The GCW is known to form within the gulf's uppermost 200 m during the late fall and winter months as a consequence of the increased vertical convective mixing induced by cold meteorological fronts (northers) which propagate from the North American Continent over the entire gulf (Elliott, 1979, 1982). The Argos 84-1 data reveal that the January 1984 northers, which had peak intensities of ~90 km h^{-1}, gave rise to a mixed layer that extended from the sea surface to a depth of 175 m. Within this mixed layer the vertical distribution of temperature and salinity were homogeneously distributed. A representative example of this phenomenon is shown in Fig. 4, where we have plotted the distribution of potential density (σ_θ) vs. depth for the easternmost hydrographic stations of each of the eleven Argos 84-1 transects. The vertical distribution of potential density clearly reveals that the average thickness of the mixed layer within the western Gulf of Mexico during January 1984 exceeded 100 m. The maximum mixed layer thickness of ~175 m is shown in Fig. 4, and was measured in Stations 6 and 7 of Transects I and II. It reveals the maximum depth of convective mixing induced by the northerly wind stress in the western gulf during our period of measurements.

The convective mixing induced by the northers within Loop Current rings erodes the static stability of their summer thermoclines. This allows for the gradual dilution of their Caribbean Subtropical Underwater (SUW; $S > 36.5$‰; $T \approx 22.5$°C) cores with lesser salinity ($S \leq 36.30$‰)

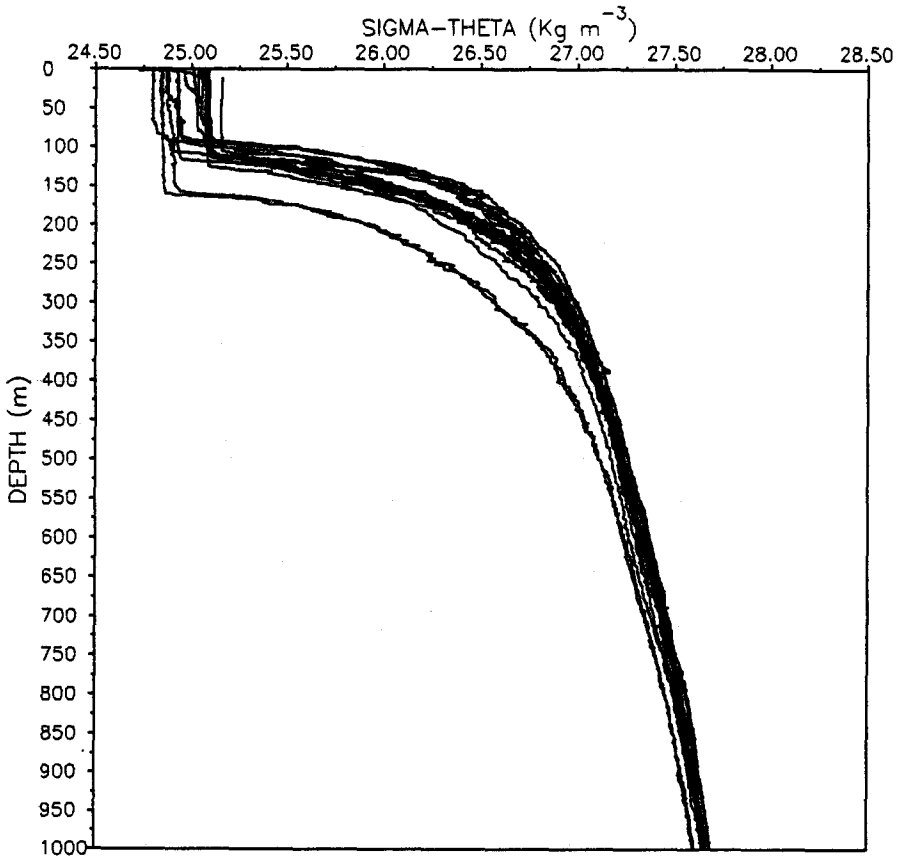

Fig. 4. Distribution of potential density (sigma-theta) versus depth corresponding to the easternmost hydrographic stations of the eleven Argos 84-1 Transects.

water from the main thermocline and, as they approach the western gulf, with continental shelf water. This is shown in Figs. 5(a), (b), (c) and 6. In Figs. 5(a), (b) and (c) we have plotted the vertical distribution of temperature, salinity, potential density, and dissolved oxygen in Station 7, during three periods of measurements: January 1984, and May and October 1987. The distribution of hydrographic properties in this station is typical of that within anticyclonic Loop Current rings in the western gulf during winter, spring, and early fall, respectively. The rings are readily identified by the presence of the SUW and its maximum salinity signature ($S \approx 36.70$‰) and temperature of ~22°C. Within the winter anticyclone's mixed layer, shown in Fig. 5(a), the GCW is overwhelmingly present with typical temperature and salinity values of 23°C and 36.38‰. The formation and evolution of the seasonal thermocline from spring to the end of summer is shown in Figs. 5(b) and (c). Its disappearance during winter, as a consequence of the convective mixing that is driven by the northers, can be deduced by comparing the magnitude of each of the mixed layers in Figs. 5(a), (b) and (c). The GCW is clearly present in Fig. 5(a) while in Figs. 5(b) and (c) the salinity distribution within the seasonal thermocline reveals values of $S \geq 36.45$‰. The salinity maximum ($S \approx 36.80$‰) that appears below the sea surface, at 47 m depth and shown in Fig. 5(c), forms as a consequence of the evaporation that results from summer heating and is thus absent during winter and spring (Figs. 5(a) and (b)). The subsurface salinity

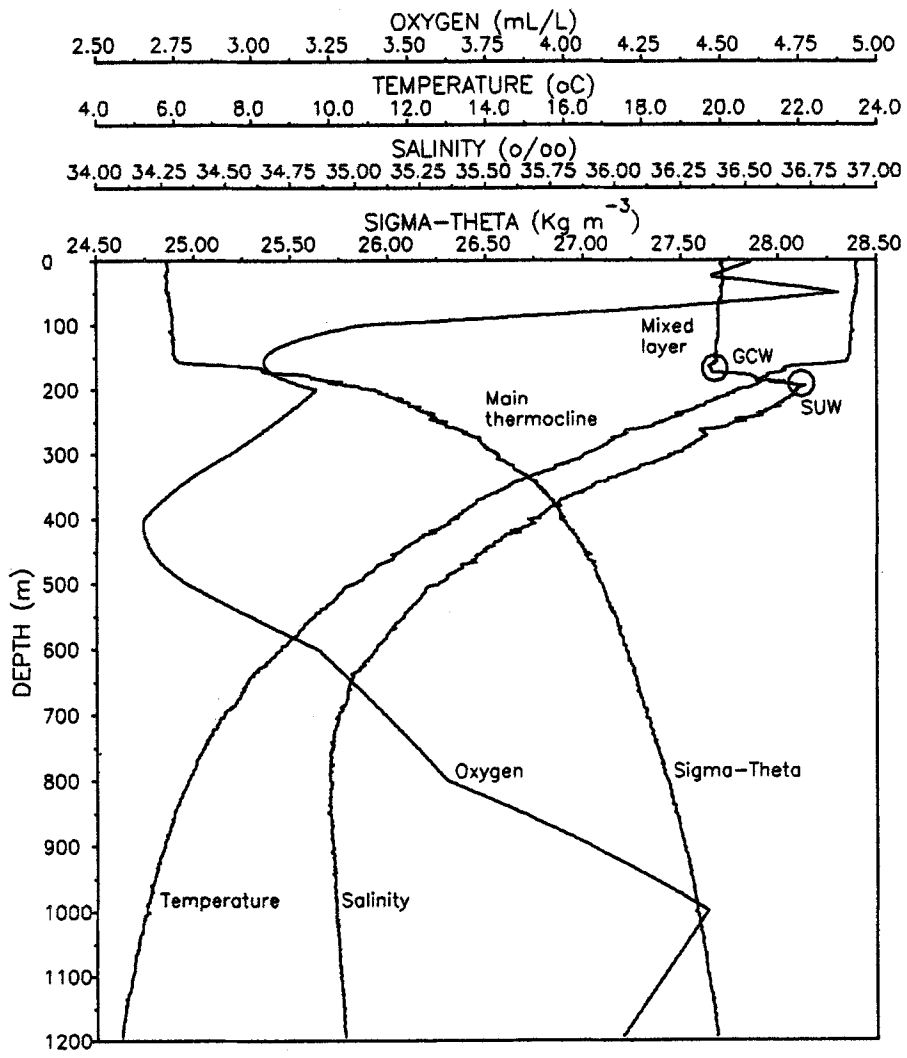

(a)

Fig. 5. Vertical distribution of temperature, salinity, potential density, and dissolved oxygen in Station 7 (25.0°N, 95.0°W) during three periods of measurements: (a) January 1984, (b) May 1987, (c) October 1987.

maximum occurs at the base of the summer mixed layer and coincides with the dissolved oxygen maximum (Fig. 5(c)).

During spring, the dissolved oxygen maximum profile appears eroded and is not as well defined as that during the early fall (Figs. 5(b) and (c)). This reflects the end of the northers season in the western gulf and the onset of diminished convective mixing which peaks at the end of the summer. The dissolved oxygen profile within the oxygen minimum layers in Figs. 5(a) and (b) show considerable variability just above the oxygen minimum layer. This variability is absent in Fig. 5(c). It results from the convective mixing that is induced by the northers and defines the

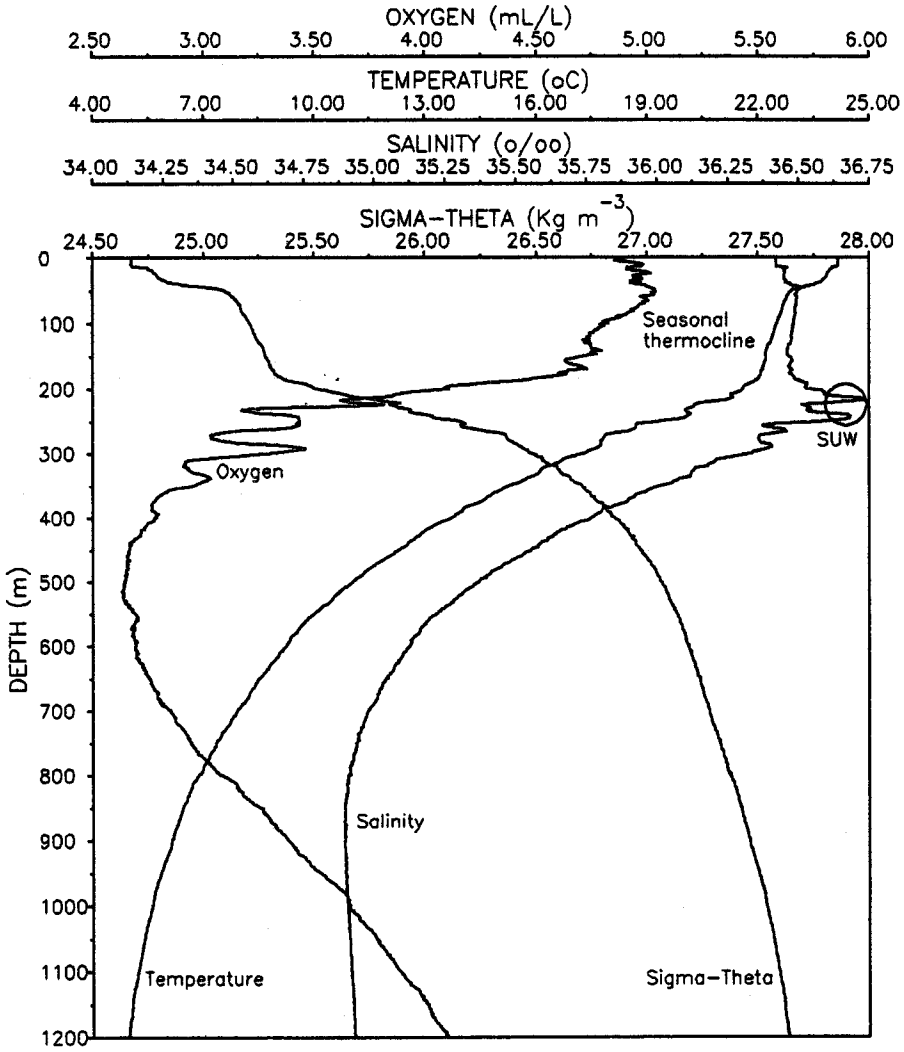

(b)

Fig. 5. (continued).

maximum depth (~300 m) of the water mass within the main thermocline that is affected by vertical mixing and contributes in the dilution of the SUW.

Figure 6 is a temperature vs. salinity dispersion diagram of all the Argos 84-1 cruise CTD data. From this *T-S* diagram one can readily deduce the mixing processes that dominate within the mixed layer of the western gulf and which form the GCW during winter. The mixing processes within the mixed layer can be deduced from the initial dispersion of the *T-S* data that is centered at $\sigma_\theta = 26.5$ mg cm^{-3} and identified by the number 1 in Fig. 6. This potential density surface is located within the main thermocline, below the base of the mixed layer. In this region, temperature and salinity have values of 16 to 17°C and 36.13 to 36.30‰. The northerly wind stress forces the mixing of this water mass with the core of the SUW, labeled by the number 2

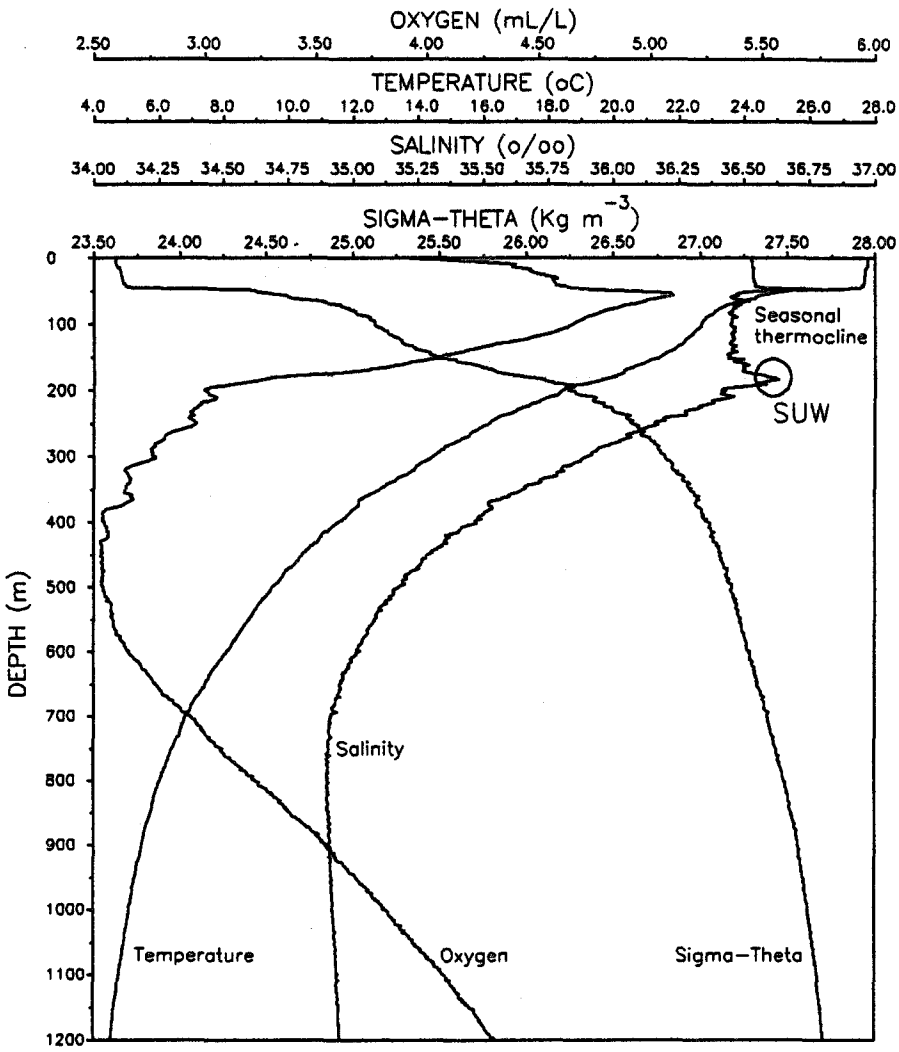

(c)

Fig. 5. (continued).

in Fig. 6. The mixing between these two water masses is clearly identified by the dilution pattern between 1 and 2. The end product of this mixture is the GCW and its core is centered at $\sigma_\theta = 25.5$ mg cm^{-3} ($T = 21°C$; $S = 36.3$ to 36.4‰) in Fig. 6. Within the oceanic region of the western gulf the core of the GCW is heated by solar radiation and attains minimum density values of $\sigma_\theta = 25.0$ mg cm^{-3}. Within the western gulf continental shelf the GCW is cooled by coastal water that has been affected by the cold norther fronts and diluted by low salinity coastal water lenses of river runoff origin. This cooling and dilution of the GCW is readily identified by the *T-S* dispersion sequence in Fig. 6.

Although the formation of the GCW in the western Gulf of Mexico is influenced by the northerly wind stress it appears from the observations of Vidal *et al.* (1985a, 1985b, 1986, 1989,

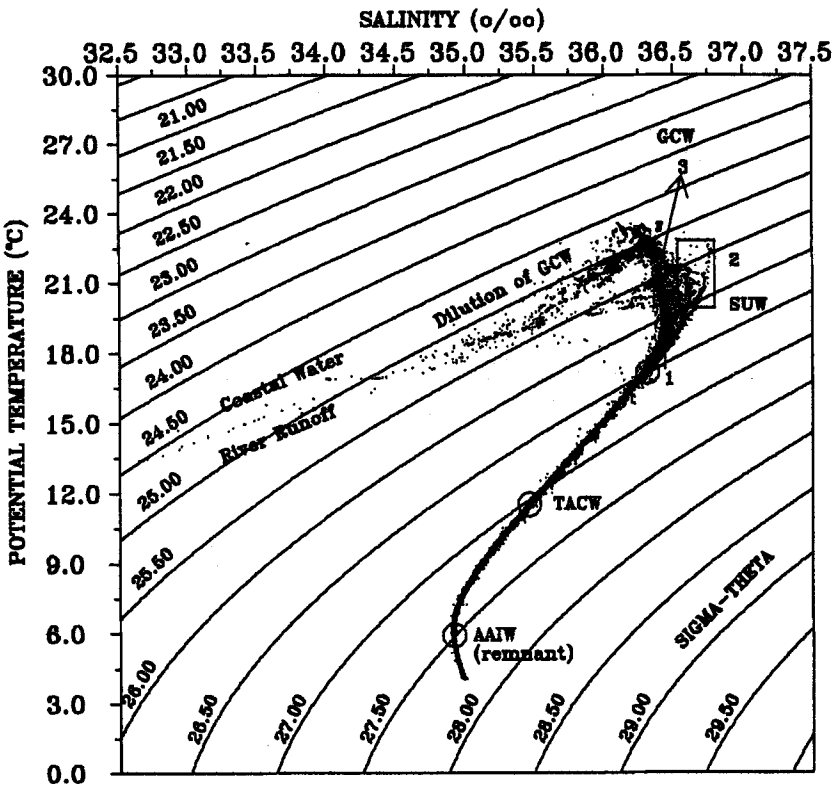

Fig. 6. Salinity versus potential temperature dispersion diagram of all the Argos 84-1 cruise CTD data. Principal water masses, within 0–1000 dbar, are identified by their temperature, salinity, and potential density relationships.

1992) that another important mechanism for GCW formation is the mixing induced by the collision of Loop Current rings against the western gulf boundary. These rings' collisions affect areas of the order of 5×10^4 km^2, wherein the SUW is diluted by lesser salinity ($36.1 \leq S \leq 36.3$‰) water from the uppermost layer of the main thermocline. The end product of this mixture is the GCW (Vidal *et al.*, 1992). The mixing mechanism that drives the GCW formation within the anticyclones' collision zones is vertical convergence, which is induced by the anticyclones' shedding approximately one third of their mass-volume ($\sim 2 \times 10^4$ km^3) to south flanking cyclones (Vidal *et al.*, 1992). The mass-volume that is shed by the anticyclones during their collision must be replenished through increased vertical advection within the anticyclones' collision zones by the surging of an equal mass-volume, to that which was originally shed, from the water mass that underlays the SUW. This is required to satisfy mass conservation and volume continuity within the colliding anticyclones. The increased vertical mixing within the anticyclones' collision zones dilutes the SUW to GCW. The SUW to GCW dilution sequence is similar to that described previously in our analysis of Fig. 6, except that the principal driving force is vertical convection driven by mass and volume continuity at the anticyclones' collision zone, rather than the vertical convection that is induced by the northerly wind stress.

The distribution of the SUW in the western gulf during January 1984 that is presented in Fig. 7 exemplifies this phenomenon. This figure represents the topography of the core of the SUW.

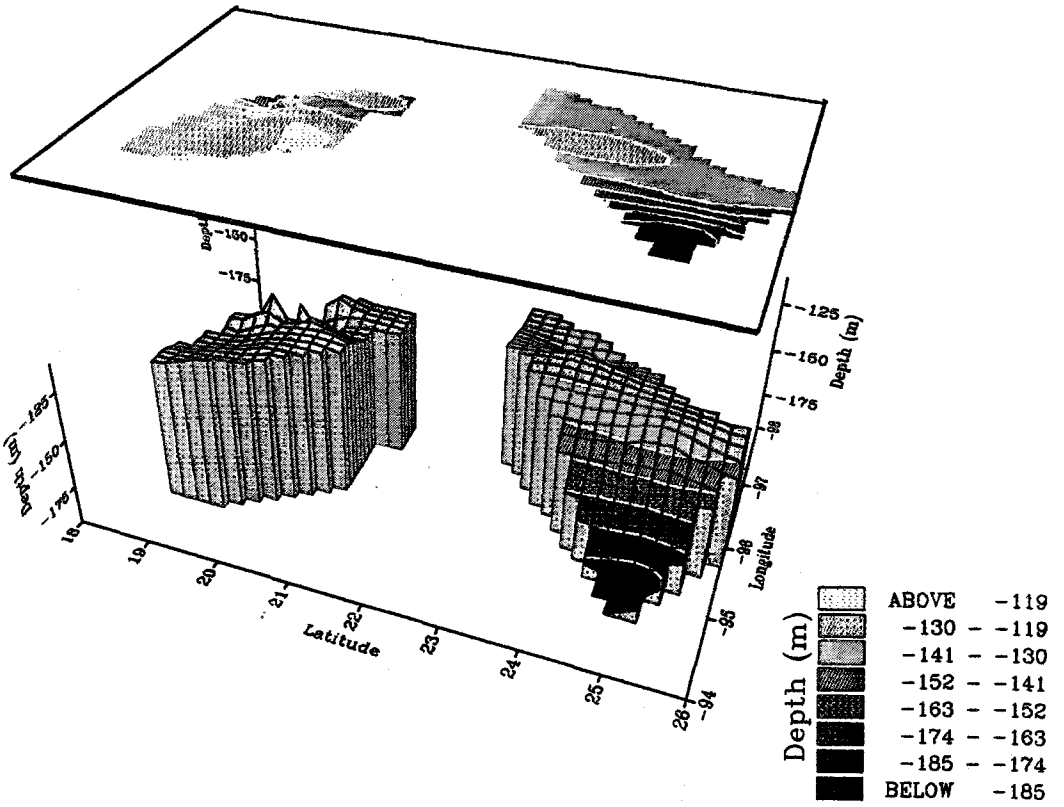

Fig. 7. Topographic distribution of the core ($S > 36.50‰$) of the Subtropical Underwater (SUW) within the western Gulf of Mexico. The maximum (195 m) and minimum (112 m) depths of occurrence are located within the anticyclonic and cyclonic domains, respectively. The SUW disappears, because of its dilution, within the anticyclone's collision zone (21.5–23.0°N) where the Gulf Common Water predominates.

It has been plotted as a function of the depth of occurrence of the salinity maximum ($S > 36.50‰$) which represents the signature that identifies anticyclonic rings in the Gulf of Mexico. The SUW is unambiguously identified in Transects I thru III. It identifies the anticyclone's domain. The SUW and its remnant are also identified in Transects VII thru XI within the cyclone's domain. The core of the SUW within the anticyclone's northwest region (Station 7) is located at a depth of 195 m. Within the cyclone, in the gulf's southwest region (Station 65), the SUW core undergoes an 83 m vertical (upward) advection and is thus located at 112 m depth. The SUW disappears, because of its dilution, in Transects IV, V, and VI, as is shown in Fig. 7. This is the region where the anticyclone's collision occurs. Within this region's mixed layer the GCW predominates. This is shown in Fig. 8, which represents a dispersion diagram of all the temperature and salinity data of the hydrographic stations contained in Transects IV, V, and VI. Only vestiges of the SUW remnant were identified in Stations 32 and 33 of Transect VI as is shown in Fig. 8.

The occurrence of the SUW tracer to the north of 23°N and to the south of 21.5°N and its

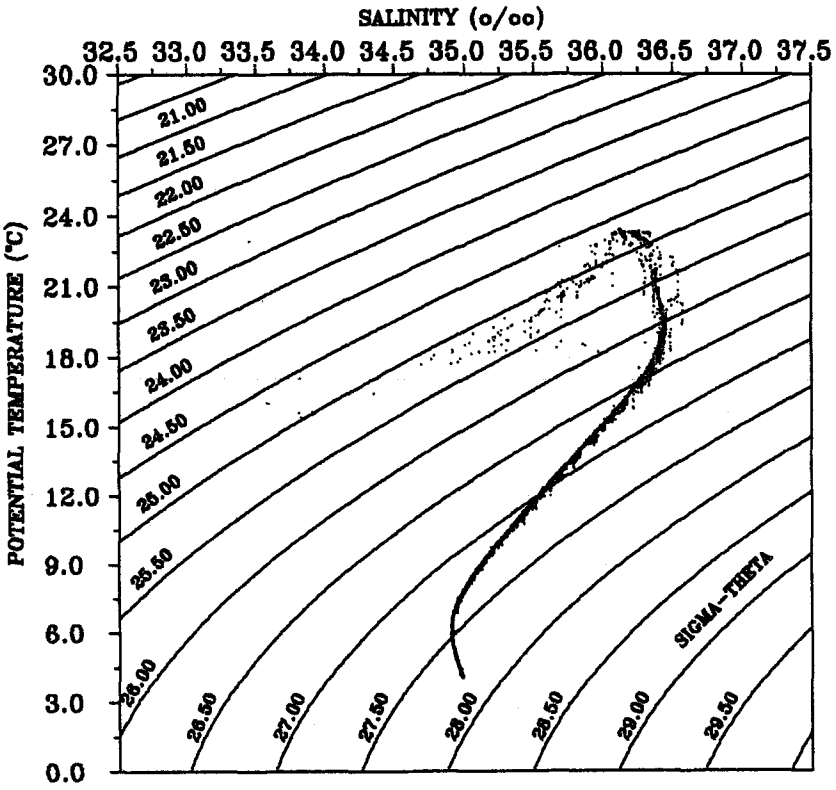

Fig. 8. Salinity versus potential temperature dispersion diagram of hydrographic data within the anticyclone's collision zone (21.5–23.0°N; Transects IV, V and VI). Within this region's mixed layer the Gulf Common Water ($\sigma_\theta = 25.5$ mg cm^{-3}, $T = 21$°C, $S = 36.3$–36.4‰) predominates. Only vestiges of the SUW ($S > 36.5$‰) are identified.

disappearance in between these two latitudinal boundaries is consistent with our model which describes the collision of anticyclonic rings against the continental slope of the western Gulf of Mexico. The SUW tracer marks the anticyclonic ring's presence off the continental slope north of 23°N. The SUW tracer also identifies water of Loop Current origin off the continental slope south of 21.5°N. This SUW water volume was shed by the anticyclonic ring during its collision and acquired its cyclonic vorticity from mass-volume conservation and lateral shear in the southward current jets that flow parallel to the gulf's southwestern continental slope boundary during the anticyclones' collision events (Vidal *et al.*, 1992, 1994).

The SUW tracer disappearance within the anticyclonic ring's collision zone and the formation of the GCW within this same area are the results of enhanced convective mixing that is driven by mass-volume continuity that results from the collision event. This convective mixing dilutes the SUW with less saline lower bounding water from the uppermost layer of the thermocline, as shown in Fig. 6. The absence of the SUW in Transects IV and V and its vestiges in Transect VI (Figs. 7 and 8) cannot be attributed to dilutive processes that are driven by the northerly wind stress. If this were true, one would expect the SUW to be diluted within the entire western gulf and not solely in the central region to the east of Tamiahua. Furthermore, one would not expect to observe the salinity discontinuity we measured in Transects IV, V, and VI given

the Lagrangian trajectory of drifter 3375 that is reported in Fig. 2(a) of Lewis and Kirwan (1985). The drifter's trajectory clearly establishes the presence of an anticyclonic ring that has been interacting, from August 10, 1983 to February 29, 1984, with the continental shelf and slope of the western gulf, between 22° to 26°N. Given the ring's presence within this area and its strong SUW signature north of 23°N, one would expect to encounter SUW within the region bounded by 21.5° and 23°N. Since this does not occur, we have to attribute the SUW disappearance and the GCW predominance within Transects IV, V, and VI (Figs. 7 and 8) to enhanced convective mixing driven by the anticyclone's collision event.

4.2 Water masses below 200 dbar

The *T-S* dispersion diagram of all the Argos 84-1 hydrographic data shown in Fig. 6 can be used to identify the water masses present below 200 m in the western Gulf of Mexico during January 1984. Within the intermediate depth of 200 to 1000 m, the straight line between $\sigma_\theta = 25.5$ and 27.4 mg cm^{-3} in Fig. 6 identifies a dilution pattern between the SUW, the Tropical Atlantic Central Water (TACW), and the Antarctic Intermediate Water remnant (AAIW).

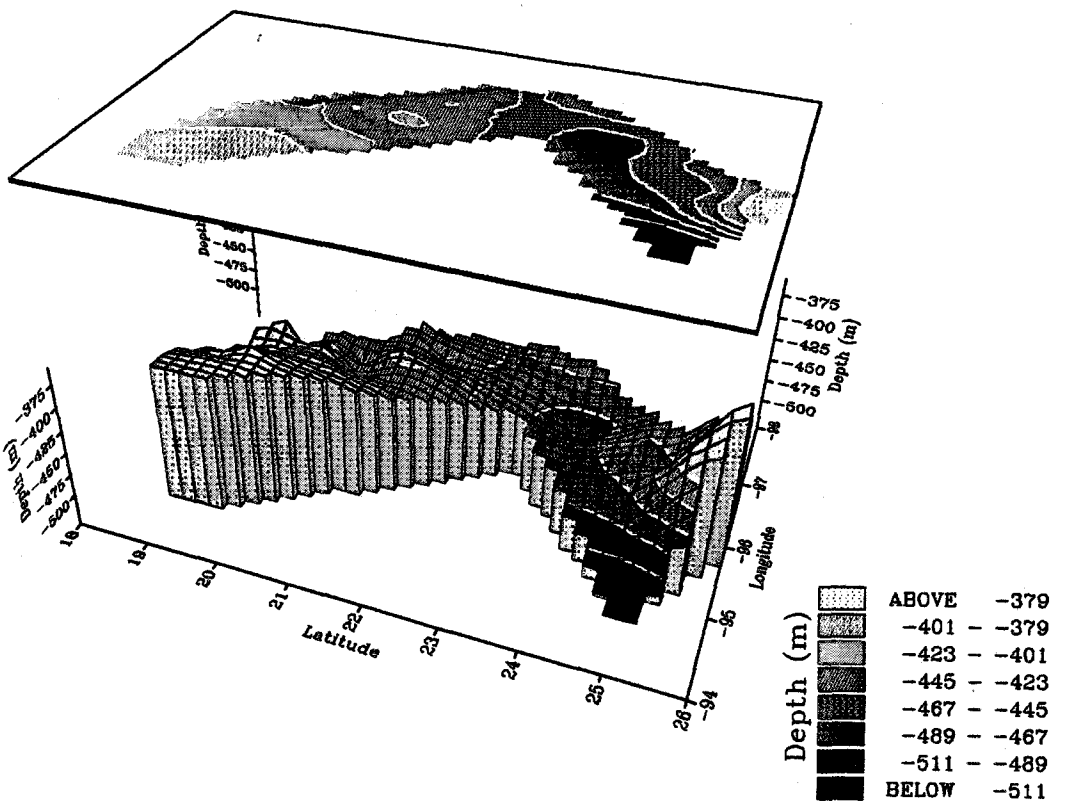

(a)

Fig. 9. Topographic distributions of (a) The Tropical Atlantic Central Water ($\sigma_\theta = 27.150$ mg cm^{-3}, $\theta =$ 10°C, and $S = 35.250$‰), and (b) the dissolved oxygen minimum core stratum (2.3–3.0 mL L^{-1}) in the western Gulf of Mexico during January 1984.

Morrison and Nowlin (1982) and Morrison *et al.* (1983) have identified the TACW in the eastern Caribbean and in the western Gulf of Mexico by its potential density surface of 27.15 mg cm^{-3}, which occurs within the oxygen minimum layer of 2.5–2.9 mL L^{-1}. We have identified the core of the TACW within the oxygen minimum layer (2.3–3.0 mL L^{-1}) of the western gulf, at a depth of 357–531 m, by the occurrence of its potential density of 27.150 (±0.002) mg cm^{-3}, and associated potential temperature of 10.08 (±0.2) °C, and a salinity of 35.250 (±0.043) ‰.

The topographic distributions of the TACW and dissolved oxygen minimum core strata in the western gulf during January 1984 are shown in Figs. 9(a) and (b). Within the anticyclonic domain, to the north of 23°N, the TACW and oxygen minimum cores are depressed. Their maximum depths of occurrence were located in Stations 5 and 7 (TACW) at depths of 500 and 531 m, respectively. Within the cyclonic domain the TACW and oxygen minimum cores underwent maximum surges of 150 m and 400 m in Stations 63 (TACW) and 67, respectively. Within the anticyclone's collision zone, 21.0° to 23.0°N, the TACW's core maximum ascent of 113 m was registered in Station 32, where its depth of occurrence was 418 m (Fig. 9(a)). Given the SUW dilution effect within the anticyclone's collision zone, one would expect the dissolved oxygen minimum stratum's core to undergo maximum surges within this region. This is indeed

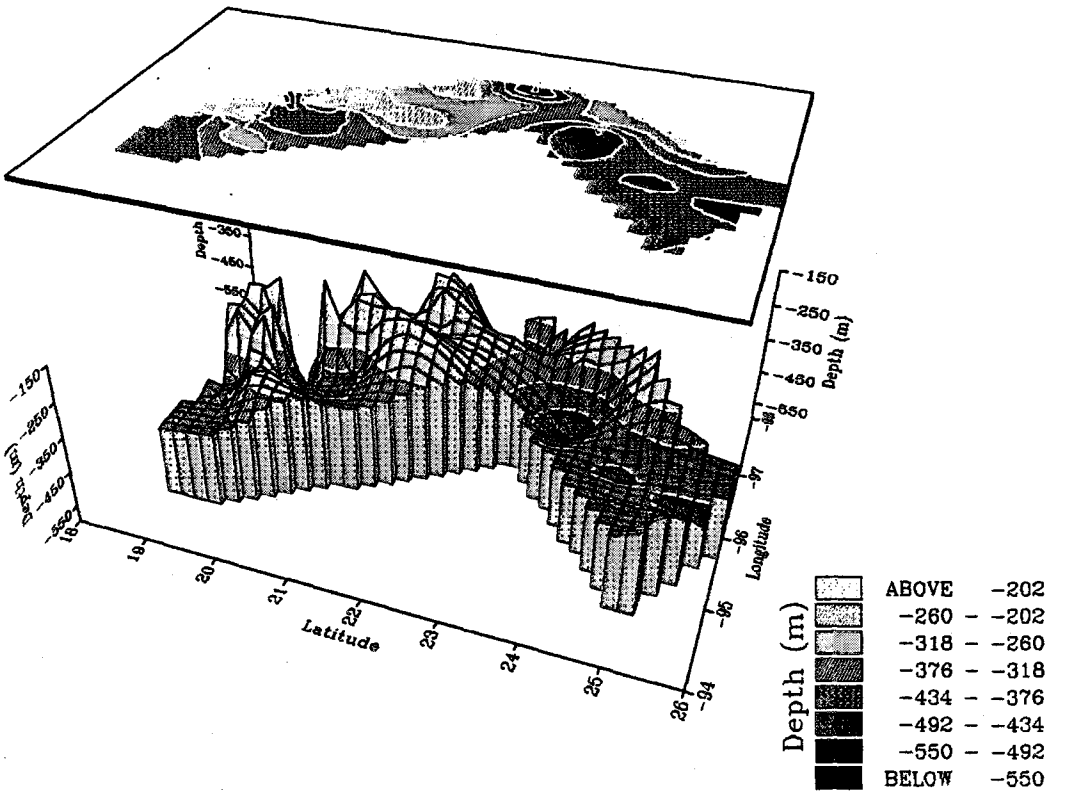

(b)

Fig. 9. (continued).

the case, as is shown in Fig. 9(b) the oxygen minimum core surges 350 m at Station 23 and 300 m in Stations 28, 29, 30, and 32, all of which are located within the anticyclone's collision zone. The topographic distributions of the TACW and oxygen minimum strata shown in Figs. 9(a) and (b) are clearly affected by the baroclinic circulation and reflect the anticyclonic ring's interaction with the western gulf continental margin.

In the Caribbean Sea, the core of the AAIW occurs at depths of 700–850 m within the potential density surfaces of 27.30–27.40 mg cm^{-3} (Wüst, 1963, 1964). Driven by the Caribbean Current the AAIW flows into the Yucatan Basin and across the Yucatan Straits into the Gulf of Mexico (Wüst, 1963, 1964). Once it enters the gulf it disperses towards the west via anticyclonic rings that are shed by the Loop Current. During its trajectory into the western gulf the AAIW increments its salinity to 34.88–34.89‰ and the thickness (~50 m) of its stratum is reduced considerably relative to that in the Caribbean (Nowlin, 1972). Within the western gulf the depth of occurrence of the AAIW remnant varies considerably (620 to 900 m) and is determined by the presence and interaction of cyclonic-anticyclonic rings (Vidal *et al.*, 1990, 1994).

Because of its dilution, the core of the AAIW in the western gulf retains only 1–2% of its original Subantarctic water mass component and is thus named the AAIW remnant (Nowlin,

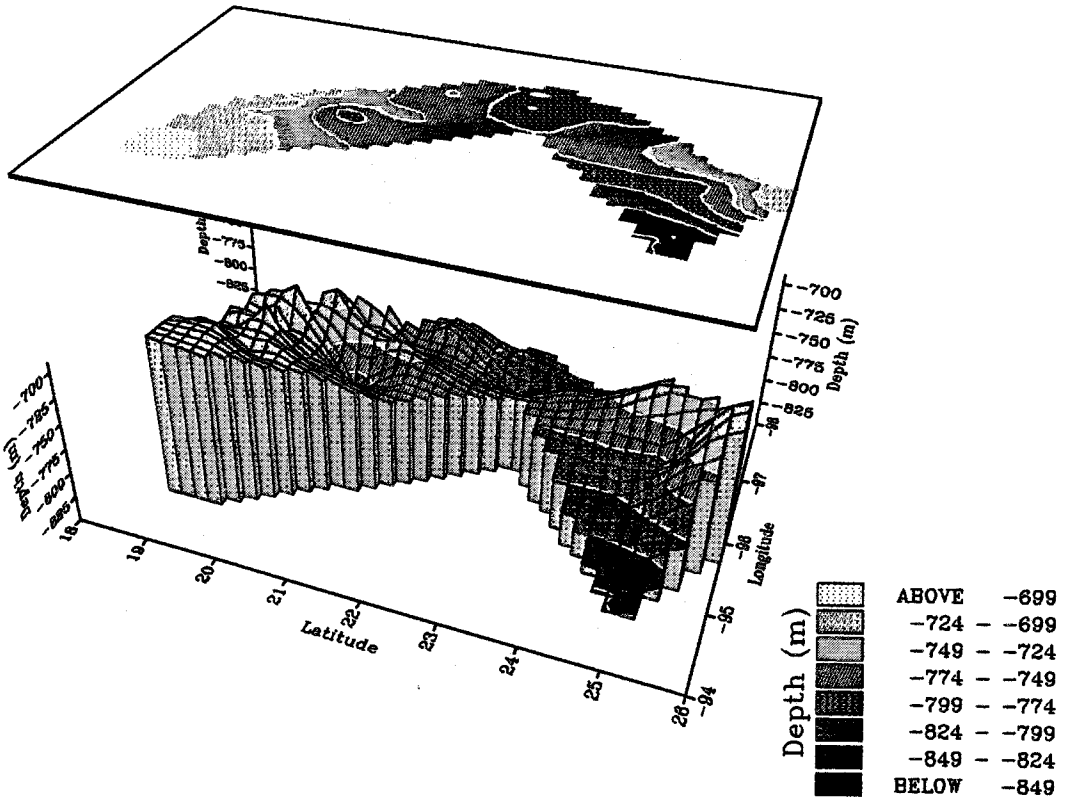

Fig. 10. Topographic distribution of the Antarctic Intermediate Water (AAIW) remnant (σ_θ = 27.40–27.50 mg cm^{-3}, θ = 5.9–6.4°C, and S = 34.878–34.908‰) within the western Gulf of Mexico during January 1984.

1972). It is unambiguously identified in Fig. 6 by the inflection in the *T-S* curve associated to the salinity minimum of 34.878–34.908‰, at 5.9–6.4°C and σ_θ = 27.40–27.50 mg cm^{-3}. The topographic distribution of the AAIW remnant within the western gulf during January 1984 is shown in Fig. 10. Its distribution is dictated by the baroclinic circulation and follows a similar pattern to that of the TACW. Within the anticyclonic domain the AAIW remnant is depressed 154 m relative to its depth of occurrence within the cyclonic domain. Its maximum depth was registered in Station 7 at 849 m. Within the cyclone the AAIW remnant was located in Station 77 at a depth of 695 m. The pressure differential between the core occurrences of the TACW and the AAIW remnant, within the cyclonic and anticyclonic domains, are practically equivalent—150 to 154 dbar—and attests to the overwhelming influence that anticyclonic ring collisions have on the baroclinic circulation and on the distributions of these two water masses in the western gulf. Their presence within the cyclone's domain, as is the case of the SUW, has to be attributed to the anticyclone's collision. It thus appears that anticyclonic rings' interactions and/or collisions in the western gulf constitute a principal mechanism that controls the occurrence and distribution of water masses in the Gulf of Mexico south of 23°N.

The mixing pattern within the deep layer below the AAIW remnant is shown in the *T-S*

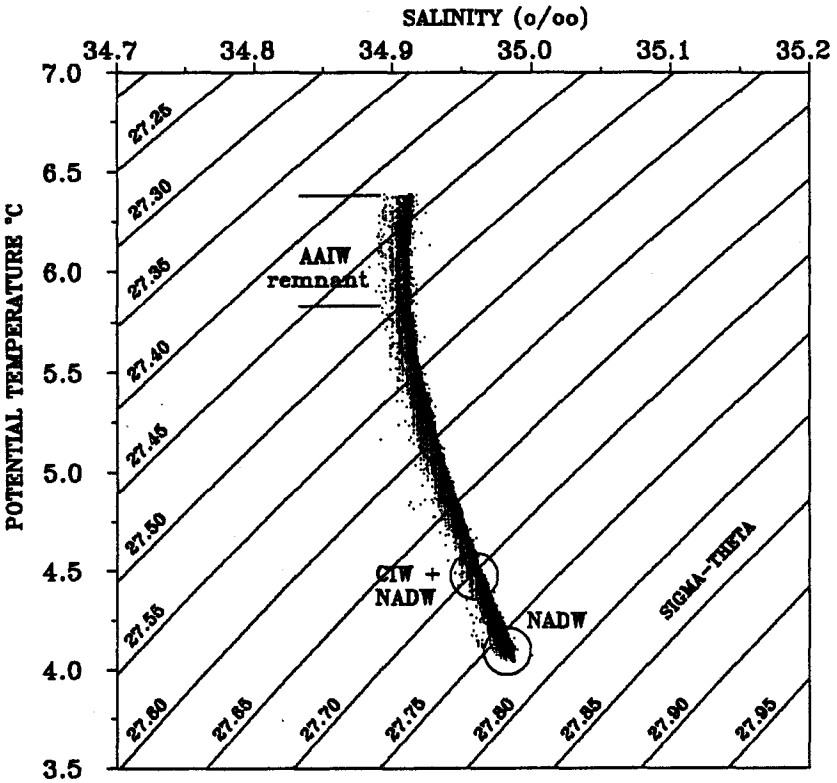

Fig. 11. *T-S* plot of all Argos 84-1 CTD deep water data describing the mixing pattern within the western Gulf of Mexico deep water layer, below the AAIW remnant. The mixture of the Caribbean Intermediate Water (CIW) and the upper portion of the North Atlantic Deep Water (NADW) is shown. The NADW is represented by the end points in the *T-S* diagram, where σ_θ = 27.750 mg cm^{-3}, θ = 4.3°C, and S = 34.974‰.

diagram of Fig. 11. From it, one can identify: (1) a mixture of the Caribbean Intermediate Water (CIW) and the upper portion of the North Atlantic Deep Water (NADW); and (2) the NADW itself, represented by the end points in the *T-S* diagram.

The occurrence of the CIW-NADW mixture within the western gulf has been reported by Morrison *et al.* (1983). They recognized its presence during April of 1978 at a depth of 1000–1100 m, at a potential density surface of 27.70 mg cm^{-3}. The core of the CIW-NADW mixture identified in Fig. 11 is characterized by a salinity of 34.958 (±0.006) ‰, a potential temperature of 4.73 (±0.15) °C, and a potential density of 26.700 (±0.003) mg cm^{-3}. The topographic distribution of this CIW-NADW mixture is shown in Fig. 12. Its distribution is similar to those of the TACW and AAIW remnant shown in Figs. 9 and 10. This topographic distribution reveals a maximum vertical migration of ~200 m between the cyclonic (997 dbar) and anticyclonic (1200 dbar) domains and is determined by the baroclinic circulation that evolves from the anticyclonic ring's collision against the western gulf continental margin.

The NADW enters the Gulf of Mexico, from the Caribbean Sea, through the Yucatan Strait sill depth of 1600 to 1900 m (Nowlin and McLellan, 1967; Nowlin, 1972). It is advected into the central and western gulf via anticyclonic ring circulations (Vidal *et al.*, 1990). We identified the upper boundary of the NADW in the western gulf at depths of 1144 to 1383 m by its hydrographic

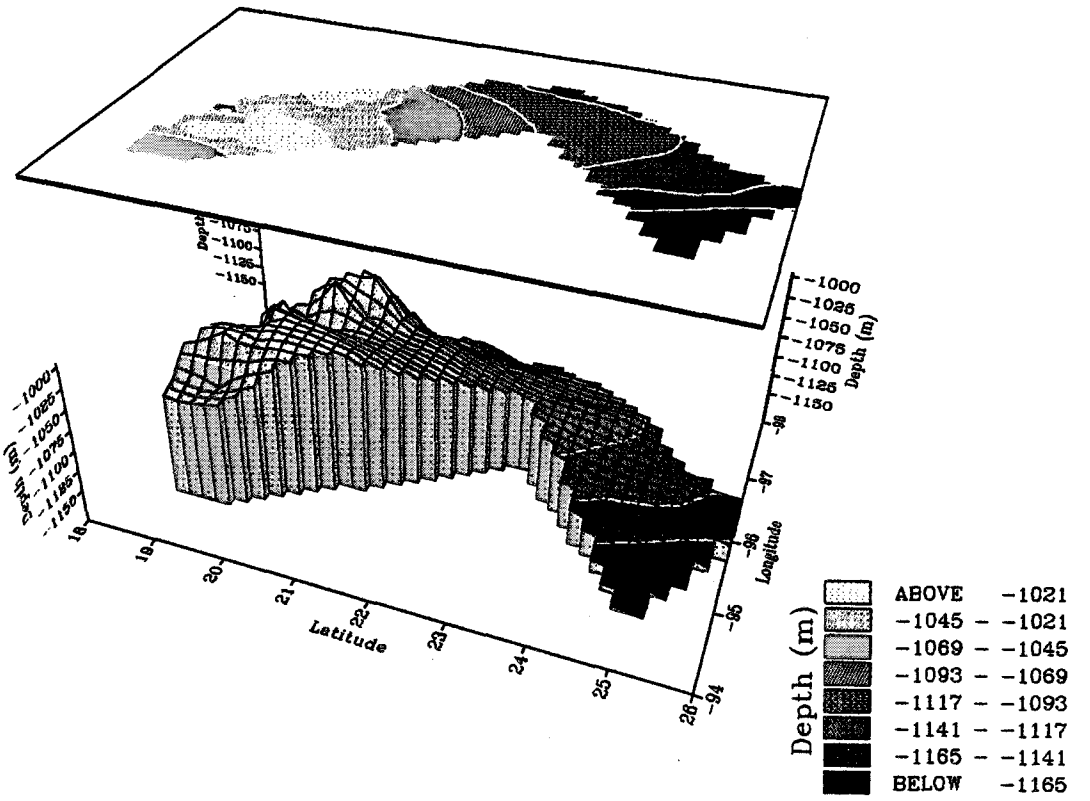

Fig. 12. Topographic distribution of the CIW-NADW mixture. The vertical migration of this water mass, between the cyclonic and anticyclonic domains, is ~200 m

signature of: $\sigma_\theta = 27.750$ (±0.002) mg cm^{-3}, $S = 34.974$ (±0.002) ‰, and $\theta = 4.36$ (±0.02) °C. The topographic distribution of this water mass is presented in Fig. 13. The cyclonic and anticyclonic circulations domains are clearly defined by the corresponding topographic high (1102 m), south of 21.5°N, and low (1383 m), north of 23.0°N. The transition zone between the cyclonic and anticyclonic domains coincides unambiguously with the anticyclone's collision zone. As would be expected, the NADW topography within this region undergoes a minimum fluctuation of only 58 m (1281–1223 m). Its vertical migration relative to the anticyclonic domain is approximately three times greater (+160 m). The maximum vertical migration of the NADW between the cyclonic and anticyclonic circulations is 281 m.

The Argos 84-1 oxygen data are summarized in the dissolved oxygen vs. potential density diagram shown in Fig. 14. This diagram includes 382 oxygen data points. The upper left cluster, centered at $\sigma_\theta = 25.0$ mg cm^{-3} and $[O_2] = 5.0$ mL L^{-1}, identifies the western gulf surface waters' concentrations. The core of the oxygen minimum layer occurs at $26.052 \leq \sigma_\theta \leq 27.37$ mg cm^{-3} and $[O_2] = 2.3$ to 3.0 mL L^{-1}. During January of 1984, this layer's depth of occurrence was localized at a depth of approximately 100 to 600 m, as is shown in Fig. 9(b). The oxygen concentrations (4.3 to 5.0 mL L^{-1}) within the deep water layer occur at $\sigma_\theta > 27.70$ mg cm^{-3} and

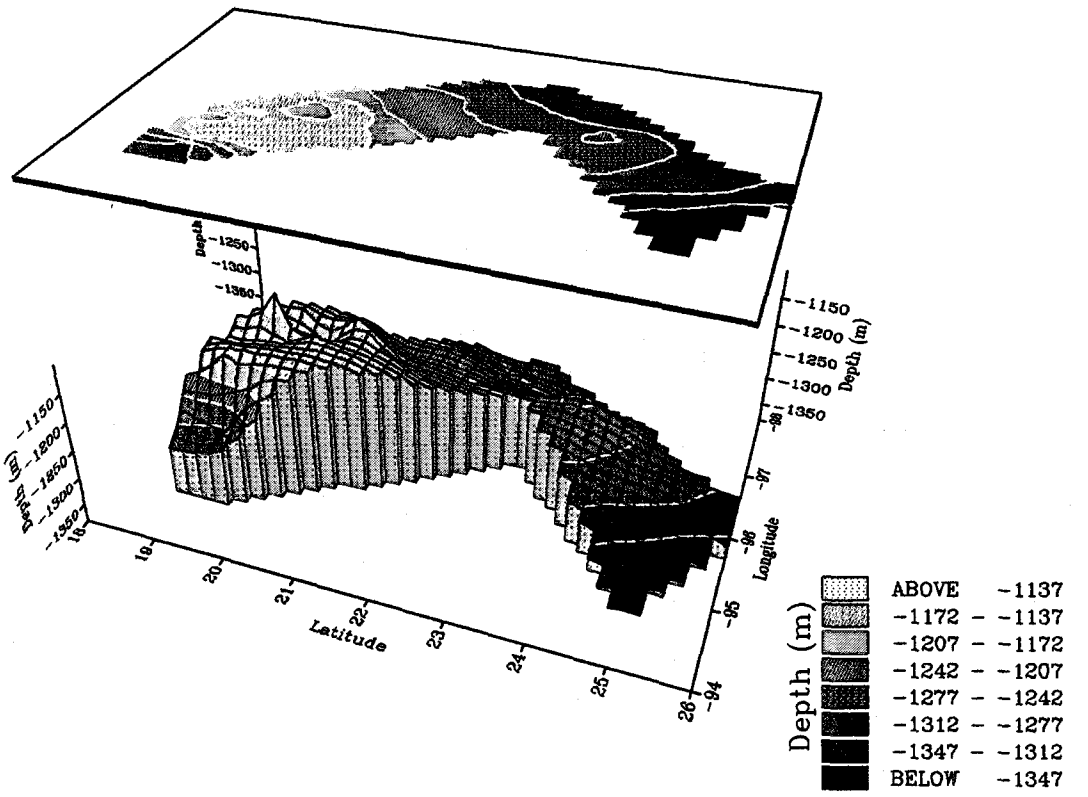

Fig. 13. Topographic distribution of the NADW ($\sigma_\theta = 27.750$ mg cm^{-3}, $\theta = 4.36$°C, and $S = 34.974$‰) in the western Gulf of Mexico during January 1984. Its vertical migration, between the cyclonic and anticyclonic domains, is 160 m.

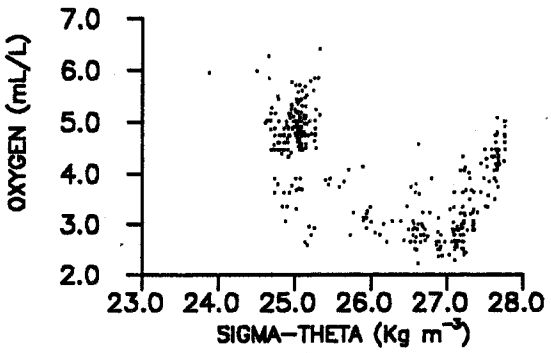

Fig. 14. Dispersion diagram of dissolved oxygen versus potential density for all bottle data collected during Argos 84-1 cruise.

characterize the NADW.

The dissolved oxygen distribution reveals a greater data dispersion within the potential density surfaces of 25.0 and 27.3 mg cm^{-3}. This dissolved oxygen dispersion occurs within the oxygen minimum layer and, as has been explained in our analysis of Fig. 9(b), is attributed to the anticyclonic ring's collision which drives the cyclonic-anticyclonic baroclinic circulation in the western gulf.

5. Sea Surface (2–3 dbar) Distribution of Hydrographic Properties

5.1 Temperature

The western Gulf of Mexico sea surface temperature distribution during January 1984 is shown in Fig. 15. The temperature range is 11.2°C. Minimum temperature values of 12.3°C were measured along the coast, from the Rio Bravo discharge to the Laguna Madre. Within the northwestern continental shelf, the horizontal temperature gradient attains a maximum value of 10°C in 110 km. This temperature gradient is associated with the cooling of the coastal water by the norther winter fronts and by the cool river water discharges contributed, primarily, by the Mississippi, Atchafalaya, and Bravo (Grande) rivers and, to a lesser extent, by the Soto La Marina and Panuco rivers (Vidal *et al.*, 1985a, 1989). Driven by the norther wind stress, these low temperature river discharges advect toward the south, hugging the coastline as is shown in Fig. 15. This observation is consistent with the work of Cochrane and Kelly (1986), who have established, from the evidence of coastal winds, current measurements, and distributions of sea surface salinity and geopotential height, that a cyclonic gyre, elongated along the Texas-Louisiana continental shelf, drives a southward flowing alongshelf circulation. This observation is also consistent with the presence of cyclonic rings off the Mexico-Texas continental shelf reported by Vidal *et al.* (1990, 1994).

To the north of Tamiahua, within Transects I through IV, the coastal water has a temperature of ~12°C, to the east of Matamoros, and 15.5°C in Station 25, that initiates Transect IV, just north of Tampico (Fig. 15). In Transects V and VI, between Tuxpan and Tampico, the sea surface water temperature increases abruptly to ~22°C. The sea surface temperature in the coastal stations of these transects is 21.85°C in Station 26 and 21.25°C in Station 38, respectively. This high surface water temperature drops to 16.85°C in coastal Station 39 that initiates Transect VII. Within

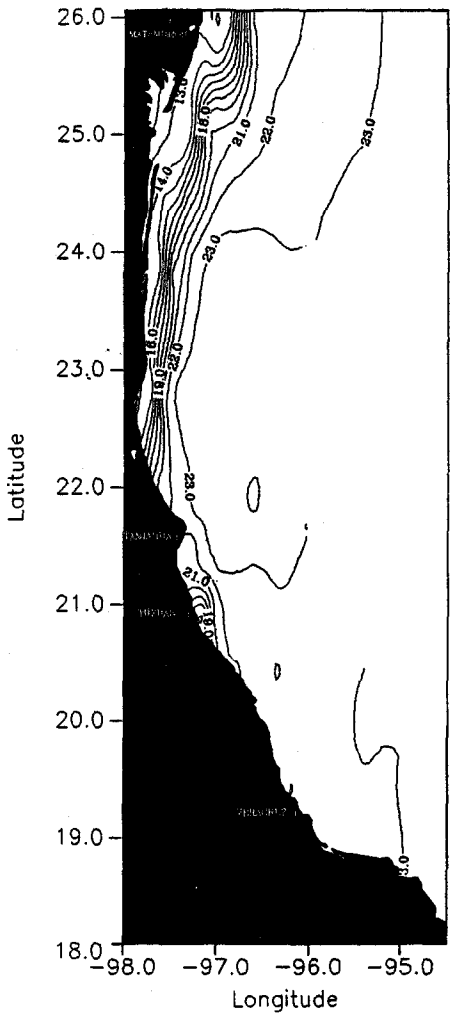

Fig. 15. Distribution of sea surface (2–3 dbar) temperature (°C) in the western Gulf of Mexico during January 1984.

Transects VIII through XI the surface coastal water has a warm 22°C temperature (Fig. 15).

The coastal and continental shelf water temperature distributions in Transects V and VI demarcate a temperature discontinuity region that coincides with the anticyclonic-cyclonic baroclinic flow transition zone, as is shown in Figs. 2(b), 3(a) and 15. Within this region, the temperature range between the surface coastal water and the oceanic water masses is only 1 to 1.5°C. Within the coastal stations of Transects IV and VII, to the north and south of the temperature discontinuity, the sea surface temperature range is 6.0–7.5°C, respectively (Fig. 15). The coastal water's temperature distribution, in Transects V and VI, indicates that the sea surface oceanic water mass intrudes upon the continental shelf at Tamiahua. As is the case with the cyclonic-anticyclonic baroclinic flow transition, this oceanic water mass intrusion, discerned from the temperature discontinuity, can be explained by the collision of the anticyclonic ring.

North of the transition zone, the ring's northern translation follows a trajectory parallel to the continental shelf slope. This oceanic, northward, baroclinic component is opposite to that over the continental shelf, which flows southward. The latter appears to be driven by the norther wind stress, which forces the low temperature coastal water to advect toward the south hugging the coastline, as is shown in Fig. 15.

South of the transition zone, the cyclone's southward baroclinic flow component and the component driven by the norther wind stress have the same sign and drive the oceanic and continental shelf water masses toward the south, respectively. Thus, the maximum sea surface temperature range between these two water masses is only 1°C. This situation contrasts markedly with the sea surface temperature distribution north of the transition zone, where the continental shelf and oceanic flows oppose each other and the maximum temperature range between the

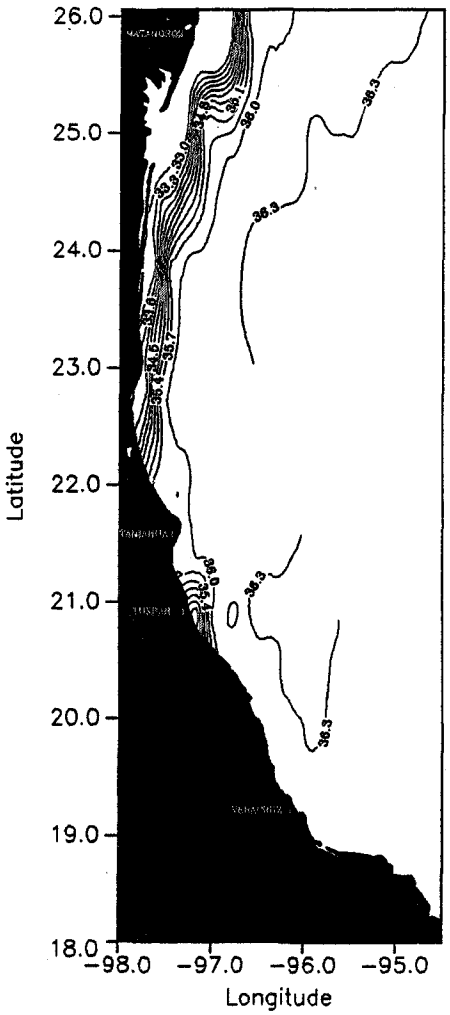

Fig. 16. Distribution of sea surface (2–3 dbar) salinity (‰) in the western Gulf of Mexico during January 1984.

oceanic and shelf waters is 10.5°C (Fig. 15). Long term current meter measurements need to be made on the continental shelf to discern the influence of the baroclinic and the wind stress driven flow components and the extent upon which the anticyclonic ring's collisions dominate the circulation over the continental shelf of the western gulf.

5.2 Salinity

The sea surface salinity distribution is shown in Fig. 16. Its distribution is strikingly similar to those of the temperature and baroclinic flow fields. As is the case with the sea surface temperature, the sea surface salinity distribution appears to be determined by the northward anticyclonic and southward cyclonic circulations and the transition zone that separates them. From Matamoros to Tampico the isohalines' orientations reveal a low salinity tongue that is

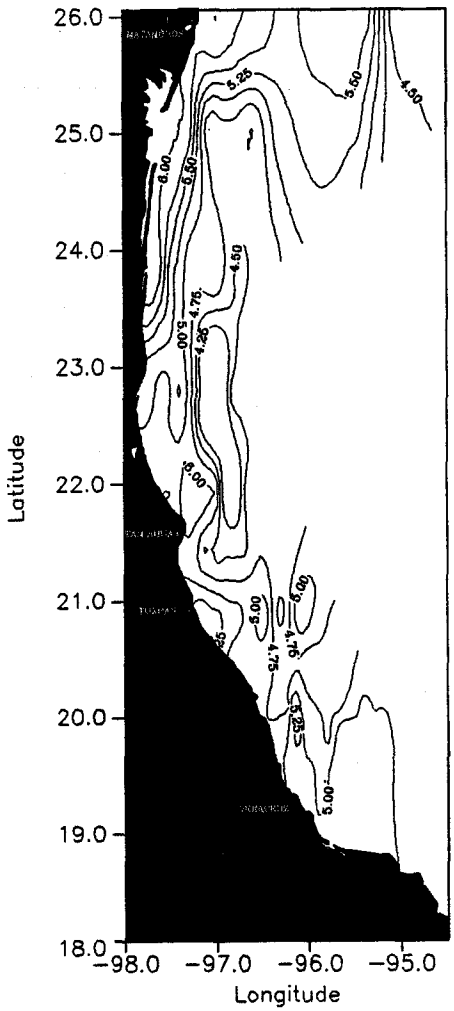

Fig. 17. Distribution of sea surface (2–3 dbar) dissolved oxygen (mL L^{-1}) in the western Gulf of Mexico during January 1984.

advected toward the south hugging the coastline (Fig. 16). The surface salinity range within the study area is 4.85‰. The minimum salinity of 31.56‰ was measured near the coast, at Station 1, to the east of Matamoros. The maximum salinity concentration of 36.41‰ was measured in the oceanic waters of Station 19 (Fig. 16). The maximum salinity gradient of 4.71‰ in ~222 km occurred along Transect I, within the anticyclonic domain. The minimum salinity gradient, of 0.36‰ in ~102 km, occurred within the anticyclone's collision zone, to the east of Tamiahua, along Transect VI (Fig. 16). The low salinity coastal waters are attributed to river runoff.

5.3 Dissolved oxygen

The sea surface dissolved oxygen distribution is similar to that of temperature and salinity and is shown in Fig. 17. It reveals a minimum concentration gradient between coastal and oceanic waters, of 0.2 mL L^{-1} in 100 km, within the anticyclone's collision zone, to the east of Tamiahua. The maximum concentration range (1.5 mL L^{-1}) between coastal and oceanic waters was measured within the anticyclone's domain. The minimum concentration of 4.5 mL L^{-1} was measured in the oceanic region, while the maximum of 6.0 mL L^{-1} was measured near the coast, to the east of Matamoros.

Given the sea surface temperature and salinity distributions, the sea surface dissolved oxygen concentrations measured reveal that the surface waters are in dynamic equilibrium with the atmosphere. The coastal maximum of 6.0 mL L^{-1}, measured east of Matamoros, reveals near saturation conditions, given the coastal water mass temperature of 12.2°C and salinity of 31.56‰. Under these conditions, the oxygen solubility concentration, at one atmosphere ambient pressure, is 6.19 mL L^{-1}. Likewise, the oxygen concentrations of 4.5 to 5.0 mL L^{-1} within the oceanic region are in dynamic equilibrium with the atmosphere, considering the average oceanic surface temperature of 23°C and average oceanic salinity of 36‰. Under these conditions, the oxygen solubility concentration, at one atmosphere ambient pressure, is 4.87 mL L^{-1} (Table 6 in Appendix of Riley and Skirrow (1975)).

6. Conclusions

Our investigations in the western Gulf of Mexico during January 1984 have allowed us to analyze the hydrographic properties and water mass distributions associated with the collision of a Loop Current anticyclonic ring against the western gulf continental slope. The dynamical aspects of the ring's collision have been reported by Vidal *et al.* (1992). The ring's collision zone has been identified from the occurrence of horizontal diverging flows, to the east of Tamiahua, that divide the surface circulation into northward (80 cm s^{-1}) and southward (26 cm s^{-1}) currents that flow parallel to the western gulf continental shelf break. This current field reveals the presence of anticyclonic and convergent flow between 23° and 26°N, and cyclonic and divergent flow to the south of 21.5°N. The transition zone, to the east of Tamiahua, reveals the region and initial stage of the ring collision. Given the unstable horizontal velocity gradients that develop within this region (21.5° 23.0°N), the baroclinic flow horizontal divergence depicts neither convergent nor divergent flow, it fluctuates from positive (2×10^{-8} s^{-1}) to negative (-2×10^{-8} s^{-1}) values. To the north and south of the collision zone the baroclinic flow stabilizes, and the horizontal divergence values become increasingly negative (-1.4×10^{-7} s^{-1}) toward the north and positive (6.0×10^{-8} s^{-1}) toward the south. Thus, the horizontal divergence distribution accurately characterizes the anticyclonic (convergent) and cyclonic (divergent) circulation properties that dominated the western gulf during and after the anticyclone's collision event.

From the distributions of the vertical component of relative vorticity at the sea surface, it

appears that the northward and southward water current jets that flow parallel to the western continental slope originate zones of high velocity shear. These zones allow the transfer of opposite sign vorticity to the water mass at the jets' western flanks. The result of this transfer of angular momentum is the formation of cyclonic and anticyclonic eddies at the western flanks of convergent and divergent water current jets, respectively.

We have studied the principal water masses' distributions in the western gulf and have found that their regional occurrences are dictated by the baroclinic circulation. This geostrophic circulation is principally determined by the presence of anticyclonic rings that are shed by the Loop Current and by their collision against the western gulf continental margin. Within the western gulf's 0–2000 m depth stratum the following water masses, listed in descending order, were identified to be present: Gulf Common Water (T = 23°C, S = 36.38‰, σ_θ = 25.50 mg cm^{-3}), Caribbean Subtropical Underwater ($T \approx$ 22°C, $S >$ 36.50‰, $\sigma_\theta \approx$ 25.75 mg cm^{-3}), Tropical Atlantic Central Water (θ = 10°C, S = 35.25‰, σ_θ = 27.15 mg cm^{-3}) and associated dissolved oxygen minimum (2.3–3.0 mL L^{-1}) stratum, Antarctic Intermediate Water remnant (θ = 5.9–6.4°C, S = 34.878–34.908‰, σ_θ = 27.40–27.50 mg cm^{-3}), a mixture of Caribbean Intermediate Water and upper portion of the North Atlantic Deep Water (CIW + NADW: θ = 4.73 (±0.15) °C, S = 34.958 (±0.006) ‰, σ_θ = 27.700 (±0.003) mg cm^{-3}), and the NADW itself (θ = 4.36 (±0.02) °C, S = 34.974 (±0.002) ‰, σ_θ = 27.750 (±0.002) mg cm^{-3}).

The topographic distribution of these water masses' strata was dictated by the cyclonic-anticyclonic baroclinic circulation that evolved from the anticyclone's collision to the east of Tamiahua. Between the cyclonic and anticyclonic domains, the maximum pressure differential of these water masses' core occurrences was 150 to 280 dbar. The topographic transition zone defined by these strata occurred between the cyclonic and anticyclonic domains and coincided unambiguously with the anticyclone's collision zone. This concordance represents an independent proof of our dynamic estimates accuracy and interpretation of the anticyclone's collision event. Thus, it appears that anticyclonic rings' interactions and/or collisions in the western gulf constitute the principal mechanism that controls the occurrence and distribution of water masses in the western Gulf of Mexico.

Our hydrographic data reveal that the January 1984 northers gave rise to a mixed layer that extended from the sea surface to a depth of ~175 m. Within this mixed layer the vertical distribution of temperature and salinity were homogeneously distributed. Our hydrographic data show that the convective mixing induced by the northers within Loop Current rings erodes the static stability of their summer thermoclines. This allows for the gradual dilution of their Subtropical Underwater (SUW; $S >$ 36.50‰) cores with lesser salinity ($S \leq$ 36.30‰) water from the main thermocline and, as they approach the western gulf, with continental shelf water. Within the winter anticyclone's mixed layer, the GCW is overwhelmingly present with typical temperature, salinity, and potential density values of 23°C, 36.38‰, and 25.50 mg cm^{-3}. Our hydrographic data collected during the three periods of measurements: January 1984 and May and October 1987, show the disappearance of the seasonal thermocline during winter as a consequence of the convective mixing that is driven by the northers.

The T-S dispersion diagram of all the Argos 84-1 cruise CTD data shows that the northerly wind stress forces the mixing of the water mass within the main thermocline centered at σ_θ = 26.5 mg cm^{-3} with the core of the SUW. The end product of this mixture is the GCW and its core is centered at σ_θ = 25.5 mg cm^{-3} (T = 21°C; S = 36.3 to 36.4‰). Within the oceanic region of the western gulf the core of the GCW is heated by solar radiation and attains minimum density values of σ_θ = 25.0 mg cm^{-3}. Within the western gulf continental shelf the GCW is cooled by coastal

water that has been affected by the cold norther fronts and diluted by low salinity coastal water lenses of river runoff origin.

Another important mechanism for GCW formation in the western Gulf of Mexico is the convective mixing that is induced by the collision of Loop Current rings against the western gulf boundary. The mass-volume that is shed by the anticyclones during their collisions is replenished through increased vertical advection by the surging of an equal mass-volume from the water mass that underlays the SUW. The increased vertical mixing within the anticyclones' collision zones dilutes the SUW to GCW. This SUW to GCW dilution sequence is similar to that described above, except that the principal driving force is vertical convection driven by mass and volume continuity at the anticyclone's collision zone rather than the vertical convection that is induced by the northerly wind stress. The distribution of the SUW in the western gulf during January 1984 justifies our conclusions. The SUW tracer marked the anticyclone's presence off the continental slope north of 23°N as well as water of Loop Current origin off the continental slope south of 21.5°N. This SUW tracer, that occurred south of the collision zone, represents the water volume that was shed by the anticyclonic ring during its collision.

The sea surface temperature range within the study area was 11.2°C. Minimum temperature values of 12.3°C were measured along the coast, from the Rio Bravo discharge at Matamoros to the Laguna Madre. Within the northwestern continental shelf, the horizontal temperature gradient attained a maximum value of 10°C in 110 km. This temperature gradient is associated with the cooling of the coastal water by the norther winter fronts and by the cool river water discharges contributed, primarily, by the Mississippi, Atchafalaya, and Bravo (Grande) rivers and, to a lesser extent, by the Soto La Marina and Panuco rivers. Driven by the northerly wind stress, these low temperature (only in winter) river discharges advect toward the south, hugging the coastline. This observation is consistent with the cyclonic circulation features reported in the works of Cochrane and Kelly (1986) and Vidal *et al.* (1990, 1994).

The coastal and continental shelf water temperature distributions demarcate a temperature discontinuity region that coincides with the anticyclonic-cyclonic baroclinic flow transition zone. The coastal water's temperature distribution indicates that the sea surface oceanic water mass intrudes upon the continental shelf at Tamiahua as a result of the anticyclonic ring collision. North of the transition zone, the norther wind stress appears to force the low temperature coastal water to advect toward the south hugging the coastline. South of the transition zone, the cyclone's southward baroclinic flow component and the component driven by the norther wind stress act on the same direction and drive the oceanic and continental shelf water masses toward the south, respectively. Long term current meter measurements need to be made on the continental shelf to discern the influence of the baroclinic and the wind stress driven flow components and the extent upon which the anticyclonic ring's collisions dominate the circulation over the continental shelf of the western gulf.

Likewise, the surface salinity distribution appears to be determined by the northward anticyclonic and southward cyclonic circulations, and the transition zone that separates them. From Matamoros to Tampico the isohalines' orientations reveal a low salinity tongue that is advected toward the south hugging the coastline. The sea surface dissolved oxygen distribution is similar to those of temperature and salinity and their concentrations reveal that the surface waters are in dynamic equilibrium with the atmosphere.

Acknowledgements

This research is part of the physical oceanography program *Estudios Oceanográficos*

Regionales del Golfo de México, sponsored by the Comisión Federal de Electricidad through contracts 862002 and 86003 and the Consejo Nacional de Ciencia y Tecnología of Mexico under grant PCCNCNA-050453 to the Instituto de Investigaciones Eléctricas (IIE). The authors would like to thank their colleagues from the Grupo de Estudios Oceanográficos at the IIE for their participation and assistance in the 1984 field program and for their collaboration in the data processing. In particular, many thanks are also due to R. A. Morales, J. M. Pérez-Molero, and J. L. Hernández for their great assistance.

References

Cochrane, J. D. and F. J. Kelly (1986): Low-frequency circulation on the Texas-Louisiana continental shelf. *J. Geophys. Res.*, **91**(C9), 10645–10659.

Cooper, C., G. Z. Forristall, and T. M. Joyce (1990): Velocity and hydrographic structure of two Gulf of Mexico warm-core rings. *J. Geophys. Res.*, **95**(C2), 1663–1679.

Elliott, B. A. (1979): Anticyclonic rings and the energetics of the circulation of the Gulf of Mexico. Ph.D. Dissertation, Texas A & M Univ., College Station, Texas.

Elliott, B. A. (1982): Anticyclonic rings in the Gulf of Mexico. *J. Phys. Oceanogr.*, **12**, 1292–1309.

Fofonoff, N. P. (1985): Physical properties of seawater: A new salinity scale and equation of state for seawater. *J. Geophys. Res.*, **90**(C2), 3332–3342.

Fofonoff, N. P. and R. C. Millard, Jr. (1983): Algorithms for computation of fundamental properties of seawater. UNESCO, Tech. Pap. Mar. Sci., 44, U.N. Educ., Sci., and Cult. Organ., Paris, 53 pp.

Fofonoff, N. P., S. P. Hayes and R. C. Millard, Jr. (1974): WHOI/Brown CTD Microprofiler: Methods of calibration and data handling. Tech. Rep. WHOI-74-89, Woods Hole Oceanogr. Inst., Woods Hole, Mass, 64 pp.

IMSL Mathematical Library (1987): *IMSL Math/Library FORTRAN Subroutines*, Vol. 2, p. 399-560, Houston, Texas.

Lewis and Kirwan (1985): Some observations of ring topography and ring-ring interactions in the Gulf of Mexico. *J. Geophys. Res.*, **90**(C5), 9017–9028.

Mantyla, A. W. (1980): Electrical conductivity comparisons of standard seawater batches P29 to P84. *Deep-Sea Res.*, **27**, 837–846.

McLellan, H. J. and W. D. Nowlin, Jr. (1963): Some features of the deep water in the Gulf of Mexico. *J. Mar. Res.*, **21**(3), 233–245.

Merrell, W. J., Jr. and J. M. Morrison (1981): On the circulation of the western Gulf of Mexico with observations from April 1978. *J. Geophys. Res.*, **86**(C5), 4181–4185.

Millard, R. C. (1982): CTD calibration and data processing techniques at W.H.O.I. using the 1978 practical salinity scale, paper presented at *International STD Conference and Workshop*. Mar. Technol. Soc., San Diego, Calif.

Millard, R. C. and N. Galbraith (1982): WHOI processed CTD data organization. Tech. Rep. WHOI-82-74, Woods Hole Oceanogr. Inst., Woods Hole, Mass, 36 pp.

Morrison, J. M. and W. D. Nowlin, Jr. (1982): General distribution of water masses within the eastern Caribbean Sea during the winter of 1972 and fall of 1973. *J. Geophys. Res.*, **87**(C6), 4207–4229.

Morrison, J. M., W. J. Merrell, Jr., R. M. Key and T. C. Key (1983): Property distributions and deep chemical measurements within the western Gulf of Mexico. *J. Geophys. Res.*, **88**(C4), 2601–2608.

Nowlin, W. D., Jr. (1972): Winter circulation patterns and property distributions, developments in the Loop Current (1969). p. 3–53. In *Contributions on the Physical Oceanography of the Gulf of Mexico, Tex. A & M Univ. Oceanogr. Stud.*, Vol. 2, ed. by L. R. A. Capurro and J. L Reid, Gulf Pub. Co., Houston, Texas.

Nowlin, W. D., Jr. and H. J. McLellan (1967): A characterization of the Gulf of Mexico waters in winter. *J. Mar. Res.*, **25**, 29–59.

Riley, J. P. and G. Skirrow (1975): *Chemical Oceanography*, Vol. 1, 2nd ed., Academic Press, London, 606 pp.

Strickland, J. D. H. and T. R. Parsons (1972): *A Practical Handbook of Seawater Analysis*. Fisheries Research Board of Canada, Bull. 167, Alger Press Ltd., Ottawa, 310 pp.

Vidal, V. M. V., F. V. Vidal, R. A. Morales, J. M. Pérez-Molero and L. Zambrano (1985a): Análisis de los datos de la campaña oceanográfica Argos 84-1 en el Golfo de México. *IIE/13/1926/I 02/P*, Inst. de Invest. Eléctr., Cuernavaca, Morelos, México, 136 pp.

Vidal, V. M. V., F. V. Vidal, J. M. Pérez-Molero, R. A. Morales, A. Rivera, L. Zambrano and R. Anaya (1985b): Hydrographic evidence for the southwest migration of a Loop Current ring in the Gulf of Mexico during January

1984 (abstract). *Eos Trans. AGU*, **66**(46), 924.
Vidal, V. M. V., F. V. Vidal, R. A. Morales and J. M. Pérez-Molero (1986): Hydrographic evidence for the collision of a Loop Current Ring in the Western Gulf of Mexico (abstract). *Eos Trans. AGU*, **67**(44), 1049.
Vidal, V. M. V., F. V. Vidal and J. M. Pérez-Molero (1989): *Atlas Oceanográfico del Golfo de México*, Vol. 1. Inst. de Invest. Eléctr., Cuernavaca, Morelos, México, 415 pp.
Vidal, V. M. V., F. V. Vidal and A. F. Hernández (1990): *Atlas Oceanográfico del Golfo de México*, Vol. 2. Inst. de Invest. Eléctr., Cuernavaca, Morelos, México, 707 pp.
Vidal, V. M. V., F. V. Vidal and J. M. Pérez-Molero (1992): Collision of a Loop Current anticyclonic ring against the continental shelf slope of the western Gulf of Mexico. *J. Geophys. Res.*, **97**(C2), 2155–2172.
Vidal, V. M. V., F. V. Vidal, A. F. Hernández, E. Meza and J. M. Pérez-Molero (1994): Baroclinic flows, transports, and kinematic properties in a cyclonic-anticyclonic-cyclonic ring triad in the Gulf of Mexico. *J. Geophys. Res.*, **99**(C4), 7571–7597.
Wüst, G. (1963): On the stratification and the circulation in the cold water sphere of the Antillean-Caribbean basins. *Deep-Sea Res.*, **10**, 165–187.
Wüst, G. (1964): *Stratification and Circulation in the Antillean-Caribbean Basins*, Part 1. Columbia Univ. Press, New York, 201 pp.